frontiers in Sensors

REVIEW
published: 20 April 2021
doi: 10.3389/fsens.2021.657931

Review: Influences of Semiconductor Metal Oxide Properties on Gas Sensing Characteristics

Bilge Saruhan[1]*, *Roussin Lontio Fomekong*[1,2] *and Svitlana Nahirniak*[1]

[1] Department of High-Temperature and Functional Coatings, Institute of Materials Research, German Aerospace Center, Cologne, Germany, [2] Higher Teacher Training College, University of Yaounde I, Yaounde, Cameroon

Semiconductor metal oxides (SMOxs) are widely used in gas sensors due to their excellent sensing properties, abundance, and ease of manufacture. The best examples of these sensing materials are SnO_2 and TiO_2 that have wide band gap and offer unique set of functional properties; the most important of which are electrical conductivity and high surface reactivity. There has been a constant development of SMOx sensor materials in the literature that has been accompanied by the improvement of their gas-sensitive properties for the gas detection. This review is dedicated to compiling of these efforts in order to mark the achievements in this area. The main material-specific aspects that strongly affect the gas sensing properties and can be controlled by the synthesis method are morphology/nanostructuring and dopants to vary crystallographic structure of MOx sensing material.

Keywords: semiconductor oxides, gas sensing, SnO_2, TiO_2, nano-structures and nanoparticles, dopants, surface loading and decoration, composites

OPEN ACCESS

Edited by:
Donatella Puglisi,
Linköping University, Sweden

Reviewed by:
Hao Cui,
Southwest University, China
Stanislav Moshkalev,
State University of Campinas, Brazil
Leonarda Francesca Liotta,
Consiglio Nazionale delle Ricerche Italiano (CNR), Italy

***Correspondence:**
Bilge Saruhan
bilge.saruhan@dlr.de

Specialty section:
This article was submitted to Sensor Devices, a section of the journal Frontiers in Sensors

Received: *24 January 2021*
Accepted: *15 March 2021*
Published: *20 April 2021*

Citation:
Saruhan B, Lontio Fomekong R and Nahirniak S (2021) Review: Influences of Semiconductor Metal Oxide Properties on Gas Sensing Characteristics. Front. Sens. 2:657931. doi: 10.3389/fsens.2021.657931

INTRODUCTION

The control and monitoring of combustion-related emissions have been the top priority of many industrial processes in view of reduced energy consumption, improvement of product quality, productivity, and environmental protection ordered by the regulations. Sensor-based intelligent systems have thus entered into the daily life and found an increased use in health and safety-related application areas, such as medical diagnostics, air-quality monitoring, food processing and detection of toxic/flammable and explosive gases, and adjustment of energy efficiency. These and other applications in harsh industrial environments require the development of fast, sensitive, selective, reliable, and also low-cost sensors. Industrial processes relied for many years on gas detection systems using infrared spectroscopy, gas chromatography/mass spectrometry (GC/MS), and chemiluminescent analysis are available with good detection limits and fast response times (Docquier and Candel, 2002). These instruments are bulky, expensive, need maintenance, and incompatible with high-temperature environments and require gas sampling systems. In the last two decades, an increased need has urged that the gas sensors are miniaturized, stable and capable of detection in a wider temperature range, highly sensitive, and selective for *in situ* monitoring at low and high temperatures and have short response and recovery times to enable feedback control under fast and repeated gas flows.

Chemical sensor technologies based on electrochemistry, calorimetry, chromatography, and spectroscopic techniques are expensive and incapable to apply for *in situ* measurements involving high temperature and chemical contaminants. Microelectromechanical systems (MEMS) offer

limited application possibility in such areas. Akbar et al. (2006) have recognized that the key technical challenge for implementation of new developed materials for chemical sensing lies in their fabrication as thin films.

Based on the pioneering work of Yamazoe (1991) on performance improvement of metal oxide (MOx) semiconducting gas sensors with nanometric crystallite sizes, many substantial efforts have been spent to produce nanostructured materials [e.g., nanoparticles (NPs), nanotubes (NTs), nanobelts, and nanowires (NWs)] demonstrating increased sensitivity and selectivity and decreased response time and operation temperature while still preserving long-term stability and reproducibility (Comini et al., 2002; Varghese et al., 2003; Kolmakov et al., 2005; Comini, 2006; Seo et al., 2009).

First introduction of MOxs as chemoresistive gas sensors was in 1952 by Brattain and Bardeen who demonstrated that some semiconductor materials modify their resistance depending on the surrounding atmosphere (Brattain and Bardeen, 1953). The conductivity changes caused by the electronic transfer in MOxs occur with the surface adsorption and desorption of gas molecules. Thus, the shape and the size of the nanostructures play a strong role in these changes. Moreover, the material characteristics, such as electronic, morphological, and chemical properties, namely band gap, Fermi level position, dispersion of catalyst, size of crystallites, and their network connection, are fundamentally required to enhance the sensitivity of sensors (Barsan and Weimar, 2001).

Metal oxides that are characterized as semiconducting transition [titanium dioxide (TiO_2), Fe_2O_3, NiO, and Cr_2O_3] and post-transition (ZnO and SnO_2) MOxs with d^{10} and d^0 electronic arrangements and smaller band gaps are good candidates to be used as gas sensing material relying on the facilitated formation of electron–hole pairs. Moreover, they offer low cost and flexible production in various nanostructured morphologies, sizes and films and simple working principle, high sensitivity, and portability (Wang C. et al., 2010).

The most common of those semiconducting MOxs that yield excellent sensing materials toward versatile gases are SnO_2 and TiO_2. Chemoresistive gas sensors based on TiO_2 emerged due to the promising features, such as reversible and large changes in the electrical resistance along with the exceptional chemical and high-temperature stability of TiO_2 (Harris, 1980). TiO_2 exists primarily in three forms: the brookite phase (orthorhombic), anatase phase (tetragonal), and rutile phase (tetragonal) with energy band gaps equal to 2.96, 3.2, and 3.02 eV, respectively. Among these crystal phases, the steady main phase is rutile, whereas the anatase phase yields better results for most gas sensor applications. In order to expand the applications of TiO_2 nanostructures in chemical sensors, there are a number of parameters that need to be improved, namely the conductance of TiO_2 in air, the sensing signal, the response and the recovery times by choosing an appropriate type, and level of doping (Zakrzewska et al., 1997; Varghese et al., 2003).

SnO_2 has been widely accepted as a suitable gas sensing material because of its low-temperature response that persists from room temperature up to a few hundred-degrees Celsius depending on detected gas type. Not the lattice oxygen concentration of SnO_2, but the chemisorbed (or ionosorbed) oxygen and other molecules with a net electric charge are critical factors for triggering a gas response. Band bending induced by charged molecules causes the increase or decrease in the surface conductivity responsible for the gas response signal. Moreover, SnO_2 is modified by additives to either increase the charge carrier concentration by donor atoms or to increase the gas sensitivity or the catalytic activity by metal additives (Batzill and Diebold, 2005).

Relying on these attractive properties, in the last two decades, especially nanostructured SnO_2 and TiO_2 have been successfully synthesized in various morphologies, in particular as 0D, one-dimensional (1D), and hierarchical three-dimensional (3D) structures, as noble metal (NM) loaded and/or bulk doped particles and layers, and their influences on the gas sensing have been demonstrated in a waste number of literatures.

This review article describes the effect of physical and chemical material characteristics, such as crystal structure, morphology and size, surface modification, and bulk doping on the gas sensors properties basing on the literature data published in the last two decades.

The particular focus is given on the most recent and important achievements related the semiconductor SnO_2 and TiO_2. The gas sensing mechanisms relevant to the target gases and sensing MOx characteristics are also highlighted. The influence of different gases on the sensing properties is explored. Although the synthesis method plays an import role in achievement of beneficial characteristics, various methods may be utilized to obtain the same or similar physical and chemical properties of semiconductor metal oxides (SMOxs). Therefore, the emphasis is given to the archived modifications in the material characteristics rather than the synthesis method.

In addition to the morphological, compositional, and crystal structural influences of the SMOxs on gas detection, the recent research indicates achievement of excellent gas sensing properties with semiconductor SnO_2 and TiO_2 through formation of composites, integration with functional materials, and building sensor arrays. With this review, it was aimed to express the achievement so far in order to grant their meaningful adoption use in future gas sensor applications.

SEMICONDUCTOR METAL OXIDE AS GAS SENSING MATERIAL

Metal oxides form the basis of the modern intellectual and functional materials and devices due to the possibility of regulating their physical and chemical properties. The functional properties of MOxs depend on many chemical and structural characteristics, including chemical composition, structural defects, morphology, grains size, specific surface area, and so on. The change of any of these characteristics allow the control of their properties. Thus, the unique characteristics of MOxs make them the most diverse class of materials with properties that cover almost all aspects of materials science and physics in the fields of semiconducting, superconductivity, ferroelectricity, and magnetism (Dai et al., 2003).

SnO_2, ZnO, In_2O_3, tungsten trioxide (WO_3), CdO, TiO_2, and other MOxs can be used as sensing material for semiconductor gas sensors. They are distinguished into a group of transparent conductive oxides due to a unique set of functional properties, the most important of which are electrical conductivity, transparency in a wide range of spectra, and a high surface reactivity. However, among the mentioned SMOxs, SnO_2, and TiO_2 are the most popular due to its manufacturability and low cost, high chemical stability, mechanical strength, heat resistance, and high adhesion to glass and other substrates.

The most important quality indicators of gas sensor performance are sensitivity, selectivity, response and recovery time, detection limit and resolution, stability, and working temperature (Bochenkov and Sergeev, 2010). These parameters of gas sensors based on SMOxs can be significantly improved by reducing the particle size to nanoscale, doping (modification) of the sensing material, and enhancement of sensor design.

Sensitivity indicates a change in the physical and/or chemical properties of the sensitive material in the presence of gas. It is determined as the ratio of sensor's resistance in the atmosphere of the target gas to its resistance in the air if the target gas is an oxidizing one:

$$S = \frac{R_g}{R_a}$$

and in the case of the reductive gas as the ratio of the device's resistance in the air to its resistance in the target gas atmosphere:

$$S = \frac{R_a}{R_g}$$

where R_g is the resistance of the sensor element in the atmosphere of the target gas, Ohm; R_a is the resistance of the sensor element in the air, Ohm (Huang and Wan, 2009; Wang C. et al., 2010).

The analytical signal can also be defined as the absolute difference between the resistance of the sensing element under the reference medium (air) and under the target gas to the resistance under the air (Ahlers et al., 2005; Dufour et al., 2012):

$$S = \frac{R_a - R_g}{R_a}.$$

The sensitivity of gas sensors is significantly affected by the porosity of the sensitive material, the operating temperature, the presence of dopants/modifiers, and the size of the crystallites (Miller et al., 2006; Wang C. et al., 2010). Given that the sensing reactions take place mainly on the surface of the sensitive material, the control of the particle size of semiconductor materials is one of the first requirements to increase the sensitivity of the sensor. Nanocrystalline materials are characterized by the highest values of the sensor signal due to the high specific surface area, and thus higher adsorption capacity (Miller et al., 2006; Sun et al., 2012; Hamanaka et al., 2016). By reducing the particle size of sensing material, it has been possible to detect H_2 at sub-ppm level (Yin et al., 2019). Furthermore, it was proven that the sensing materials based on NPs of TiO_2 offer perspectives for humidity detection even at room temperature (Dubourg et al., 2017) and high selectivity and response toward H_2S, CH_3OH, and C_2H_5OH gases (Arafat et al., 2017) at lower temperatures. Thus, sensors were achieved that exhibit excellent mechanical stability, fast response/recovery times, and good reproducibility, with minimal energy consumption and low weight.

Selectivity characterizes the ability of the semiconductor layer to distinguish the group of target gases or single gas in the gas mixture (Bochenkov and Sergeev, 2010). To increase the selectivity of gas sensors, surface modification or bulk doping with various catalytic additives is used for better adsorption of the target components (Shamsudin et al., 2002; Salehi, 2008; Liang et al., 2014; Woo et al., 2016). Previous literature demonstrate that sensing materials based on SnO_2 and TiO_2 nanostructures yield high selectivity sensors through either their surface modification with NM loading or bulk doping with redox capable elements thus facilitating the selective gas detection in mixed gas environments. These studies indicate that the improvement of sensing performance in such cases is due to the creation of new active centers on the MOx surface or changing the electronic structure of material (Saruhan et al., 2013, 2016; Liu Y. et al., 2017; Majhi et al., 2018; Yin et al., 2019; Raza et al., 2020).

Stability or reproducibility is the ability of the gas sensors to provide repeatability of measurement results for the prolonged usage. The preheat treatment at temperatures above the sensor operating temperatures improves the stability of the sensitive layers.

Response time determines the period during which the parameter value changes by a certain percentage of its initial value at the certain gas concentration.

The shortening of the response time can be achieved by the doping of MOxs with NMs. Thus, Choi J.-K. et al. (2010) demonstrated that Pd-doped SnO_2 sensing material shows response time $<$10 s. Dong et al. (2011) found that response time of 0.08 wt.% Pt-doped SnO_2 nanofibers to H_2S is much faster (1 s) than response time of the undoped SnO_2 nanofibers (2–7 s).

Recovery time is the period required for sensor to come back to its initial value after decreasing of target gas concentration to zero. The long recovery time is associated with slow surface reactions and can be accelerated by the doping of metal catalysts, such as Pd and Ag. For instance, Pd-doped (0.4 wt.%) SnO_2 hollow nanofibers exhibit significantly shortened recovery time under the exposure of H_2, CO, CH_4, and C_2H_5OH (31.8, 23.7, 38.5, and 88.5 s, respectively). In this case, the increase in recovery time can be explained by the Pd catalytic promotion of the oxygen adsorption (Choi J.-K. et al., 2010).

Both response and recovery times depend on the working temperature. Fields et al. (2006) developed the SnO_2 single nanobelt-based sensor for the hydrogen detection and found that with the increasing of the sensor operation temperature to 80°C, the response time decreases from 220 to 60 s, whereas recovery time increases more than double. Landau et al. (2009) investigated the temperature influence on sensing characteristics and found that the sensitivity of TiO_2 nanofibers to NO_2 decreases with the temperature growth, whereas response time

decreases with the increasing of temperature and decreases with the increasing of NO_2 concentration.

Detection limit is the lowest gas concentration that can be detected by sensor element. The lowest concentration difference, which can be recognized by sensor, corresponds to the *resolution* of the device. *Working temperature* of sensor is the temperature at which sensor shows the maximal sensitivity (Bochenkov and Sergeev, 2010).

Besides characteristics of the sensitive material, schematics of sensors, their design, and dimensions play a significant role in the improvement of sensor performances (Nahirniak and Dontsova, 2017).

For instance, sensitivity, selectivity, and response time are temperature-dependent parameters as the surface adsorption/desorption processes and change in the energy to activate them are affected by the sensor operating temperature (Partridge et al., 2009). In turn, working temperature, power consumption, and temperature uniformity depends strongly on the material of heater and its thickness. The highly effective gas sensor shall provide minimal power consumption and heat losses. The study of three different metals (platinum, titanium, and tungsten) for heater production by Souhir et al. (2016) showed that the platinum has the biggest prospects as it provides good compromise between high temperature and power consumption. The power consumption can be reduced by decreasing the thickness of heating electrode and the decreasing of the inter track in the design of heater that leads to the better temperature homogeneity.

The other structural element of the MOx sensing element, which cause strong effect on the gas sensing characteristics, are electrodes, namely electrode geometry and gap size. The varying of the gap size of electrodes leads to the changes in the resistance of device and consequently in the sensitivity. Shaalan et al. (2011) studied the influence of gap size of SnO_2 sensor on the NO_2 detection and have concluded that the choice of the gap size of electrode depends on the concentration of detected gas. Thus, they showed that large-gap electrode sensors highly sensitive to the high NO_2 concentration. On the one hand, the reducing of the gap sizes of electrodes improves the selectivity of sensing element to lower gas concentrations.

On the other hand, the improvement of selectivity can be achieved by the increasing of line width of electrodes. Miyaji et al. (2004) investigated the influence of electrode width and showed that sensor with bigger electrode width (50 μm) characterized by higher sensitivity compared to the sensor with electrode width of 10 μm.

Sensing Mechanism

The mechanism of analyte detection by sensitive semiconductor material can be described as follows: oxygen adsorption on the sensitive layer surface, electron transfer from material to oxygen, analyte adsorption, chemical reaction, electron transfer to the semiconductor, and desorption of the products.

The oxygen adsorption includes both physical and chemical process. Besides oxygen, water molecules and hydroxide groups are also adsorbed on the MOx surface. However, due to the high affinity to the electron, oxygen plays the main role in sensing mechanism. Depending on the temperature, oxygen can be present in the molecular (O_2^-) or atomic (O^- and O^{2-}) form. The molecular oxygen form can be found at the temperature below 150°C, whereas above 150°C the atomic forms exist (Barsan and Weimar, 2001; Tricoli et al., 2010; Krivetskiy et al., 2013):

$$O_{2gas} + e^- \rightarrow O^-_{2ads}(80^\circ\mathrm{C} - 150^\circ\mathrm{C}),$$

$$O^-_{2ads} + e^- \rightarrow 2O^-_{ads}\ (150^\circ\mathrm{C} - 260^\circ\mathrm{C}),$$

$$O^-_{ads} + e^- \rightarrow O^{2-}_{ads}\ (300^\circ\mathrm{C} - 500^\circ\mathrm{C}).$$

The adsorbed oxygen species trap electrons and form a depletion layer, which causes changes in the electrical conductivity of the sensing layers. For instance, Saruhan et al. (2013) investigated the sensor response of TiO_2 layers to NO_2 and concluded that sensor behavior under the NO_2 exposure depends on the partial oxygen pressure. At temperatures above 500°C, NO_2 becomes thermodynamically unstable, which leads to the presence of excessive oxygen sub-ions in the system. The oxygen ions form an O^-_{ads} layer, which decreases the sensor conductivity and lowers the desorption kinetics. This results in an unstable response and longer recovery time.

Depending on the charge carrier, two main types of semiconducting MOx materials are reported in the literature: p-type, where the charge carriers are the holes, and n-type, where the charge carriers are electrons. In fact, the charge carriers in wide band gap oxide semiconductors are determined either by doping aliovalent cations or by oxygen non-stoichiometry. For example, since the formation of oxygen vacancies follows the generation of electrons, undoped oxygen-deficient TiO_2 shows n-type semiconductivity. Meanwhile the deficiency of metal ions in undoped CuO explained its p-type semiconductivity. Pristine TiO_2 and SnO_2 are n-type semiconductors. Since in the ambient atmosphere, the oxygen non-stoichiometry is constant at fixed temperature, the doping of TiO_2 and SnO_2 with higher and lower valency cations can be used to control the nature and the concentration of their charge carrier (Patil et al., 2015; Dey, 2018; Ji et al., 2019).

Sensing Mechanism of N-Type MOx

The gas sensing mechanism of MOxs is fundamentally a surface-related issue resulting in a change in sensor resistance that is tightly related to the adsorption or desorption processes of target gases. As early as 1988, Romppainen described the possible occurrence principles of the sensing mechanism with n-type SMOxs (Romppainen, 1997). According to him, the surface conductivity being the main defining factor for the sensing mechanism will be influenced by the following processes:

- Oxidation/reduction of the semiconductor: the charge carrier concentration and electron structure of the sensitive materials affects by the gas concentration due to the change of the surface or bulk stoichiometry.
- Ion exchange: the change of ions leads to the formation of the surface layer with the other electron structure in comparison to the base material.

- Gas adsorption: the molecule of gas adsorbs on the surface of the material and either donates electrons to the conducting band or acts as a trapping center.
- Reaction with adsorbed species: the adsorbed gas species react with oxygen previously adsorbed on the surface resulting in lowering number of trapped electrons on the surface.

After the n-type nanostructure is exposed to air, oxygen molecules are adsorbed on the surface. Due to the electrons transfer from the semiconductor powder to the surface, the development of potential barriers on the particle surface occurs, which affects in relatively few oxygen adsorption sites available on the n-type semiconductor surface. For conductance, electrons must pass over this surface barrier to move from one particle to the next (Morrison, 1987). Depending on the temperature, adsorbed oxygen ion species (O_2^-, O^-, and O^{2-}) are formed by the extraction of conduction band electrons and by generating a space charge conduction area. This causes an increase in sensor resistance. When the target gas is injected, it is adsorbed on the material surface and then gets oxidized if the gas is a reducing gas resulting in the return of electrons back to the conduction band. As a consequence, this reduces the space charge width and the resistance proportional to the concentration of analyte. When the gas is an oxidizing one, it gets reduced by taking electrons from the conduction band, leading to the proportional increase of the resistance (Govardhan and Grace, 2016; Degler et al., 2019). Thus, in the case of n-type semiconductors, the presence of reducing gases causes the conductivity increase, and oxidizing gases decrease the sensor conductivity.

Sensing Mechanism of P-Type MOx

Compared to the n-type MOx sensors, for p-type semiconductors, the sensing mechanism in accordance to the resistance change is opposite. **Figure 1** shows the change in sensor resistance of n- and p-type MOx gas sensors upon the exposure to the reducing gas. The adsorption of oxygen molecules following by their ionization generates a hole accumulation layer on the material surface and thus resulting in a decrease of resistance. Upon exposure to a reducing gas, the target molecules react (*via* oxidation) with the adsorbed oxygen species on the surface, leading to the release of the trapped electrons back to the conduction band, which then increases the sensor resistance as a result of the hole accumulation layer becoming thinner. If the target gas is an oxidizing one, it will get reduced by taking electrons from the conduction band and thus resulting in the decrease of resistance (Kim and Lee, 2014; Wei et al., 2020).

Influence of Temperature and Humidity on Sensing Performance

The gas sensors based on SMOxs usually work at high temperature ($\geq$150°C), and their response strongly depends on the temperature. In fact, the detection of specific gas depends partially on adsorption phenomena and precisely on the thermodynamic of gas adsorption on the surface of semiconductor materials, which is related to temperature. For a given sensor, the highest response for a specific gas is obtained at a specific temperature, where the equilibrium is reached between the adsorption and desorption rate. In addition, the activation energy of the reaction taking place during the detection is reached at an optimum temperature, then the optimization of the sensor working temperature by the detection of a target gas is usually used to enhance the selectivity. An example given by Liu et al. (2015) is presented in **Figure 2** showing the response of gas sensors based on pure TiO_2 and TiO_2 NPs doped with tungsten to 3,000 ppm butane at different temperatures. As displayed in **Figure 2**, the sensitivity of sensors varies strongly with the working temperature. For instance, TiO_2 doped with 5 and 7.5% tungsten yield the highest response at 420 and 440°C, respectively (Liu et al., 2015).

In general, the response and recovery times of a sensor depend also on the temperature because the kinetic reactions between semiconductors and gases are temperature dependent. Then, at the low temperature, sensors have a long response and recovery times because the kinetic reaction rate is low (Eranna, 2012).

The water vapor, which reacts as a reducing gas, can strongly affect the base line and the sensitivity of the sensor. The change in the water vapor quantity on the surface of semiconductors can influence the sensor performance during its work. For MOx sensors, the liability is guaranteed at relative humidity superior to 10% at operating temperature of 20°C. The base line and the sensibility can be affected by the humidity below this value. To explain the influence of water vapor, two considerations can be done. First, in the presence of humidity, the adsorption of water vapor reduces the number of the available adsorption sites, which reduces the number of the adsorbed oxygen species on the surface of semiconductor. The second thing is that the water vapor can also react as electron donors to the semiconductor and this will change its base line resistance. The presence of water molecules can also create OH sites on the surface at a specific operating temperature, and this can influence the response (Wang C. et al., 2010). H_2O can be adsorbed on the Sn_2O surface as a result of physisorption or chemiosorption processes. In the first case, H_2O adsorbed in the molecular form at low temperatures, and in the second case, H_2O adsorbed in ionized form at higher temperatures. Thus, at temperatures above 400°C, water molecules are adsorbed in the MOx surface in the form of OH^- groups, which acts like electron donors. In the case of the reducing gas detection, the reaction of water molecules with the MOx surface leads to the release of the captured electrons, which causes to the decrease in resistance of sensor (Haidry et al., 2015).

In general, the adsorption of the water leads to the significant decrease of gas sensitivity. For instance, Qi et al. (2008) developed Sm_2O_3-doped SnO_2 sensor and investigated its sensor response to C_2H_2 at the humidity content in the range 11–95%. **Figure 3A** displays that sensor response decreases with the increase of humidity. Moreover, authors found out that humidity slows down with the response and recovery times. In this case, water molecules can act as barriers against gas adsorption. **Figures 3B,C** shows the gas sensing mechanism of Sm_2O_3-doped SnO_2 sensors to C_2H_2 in the humidity environment indicating that in the humid medium, the C_2H_2 migration on the SnO_2 surface becomes difficult that leads to the decrease of the sensitivity and increase of response/recovery time.

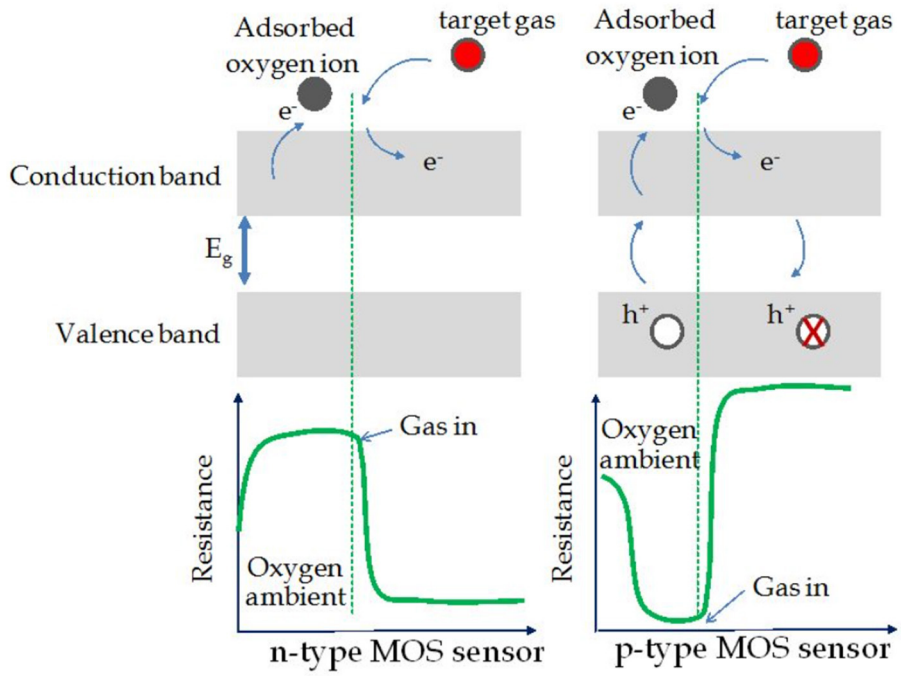

FIGURE 1 | Schematic diagram for change of the sensor resistance upon exposure to the target gas (reducing gas) in the cases of n-type and p-type MOx sensors (Reproduced from Choopun et al., 2012).

INFLUENCING FACTORS OF PHYSICAL AND CHEMICAL MATERIAL CHARACTERISTICS

Nanocrystalline materials were reported to yield good responses with the highest sensor signal values relying on their high specific surface area leading to higher adsorption capacities (Miller et al., 2006). Yin et al. (2019) have synthesized highly sensitive hydrogen sensors based on SnO_2 NPs and reported that the reduction of the particle size of the sensitive material allows to obtain sensors for the H_2 detection at sub-ppm level. In another work, it was shown that the achievement of high sensing characteristics, excellent mechanical stability, fast response/recovery time, and good repeatability when the TiO_2 NPs were employed as the sensing material for the fabrication of room temperature humidity sensors (Dubourg et al., 2017).

The parameters of gas sensors based on MOxs (stability, sensitivity, selectivity, and response time) can be significantly improved by reducing the particle size to nanoscale. The reduction in grain size to the nanoscale is one of the most effective strategies for the enhancement of the gas-sensing properties. The grain boundary barriers provide the predominant impact of gas on the conductivity of the sensor leading to the absolute control of sensing mechanism. This condition relies on the depletion layer, encapsulating each grain or grain chains and the formation of grain boundaries between those as shown in **Figure 4A** (Sun et al., 2012). On the contrary, the sensitivity of the sensing material will be independent on the grain boundaries, but controlled by the grain size. For the grains with $D \geq 2L$,

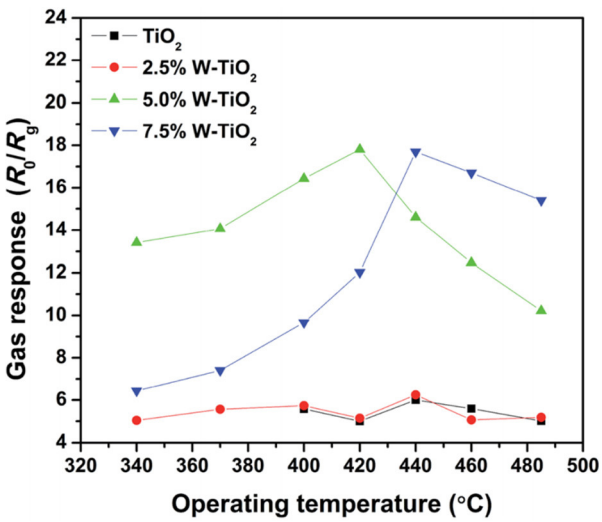

FIGURE 2 | Gas response of sensor based on TiO_2 and W-doped TiO_2 nanoparticles to 3,000 ppm butane at different temperatures (Reproduced from Liu et al., 2015).

the space–charge layer around each neck formed a conduction channel as illustrated in **Figure 4B**. The cross-sectional area and the grain boundary barriers affect the conductivity and thus resulting in enhanced sensitivity. In case of fully depletion of the grains with mobile charge carriers, the conduction channels between the grains become mislaid and conductivity decreases

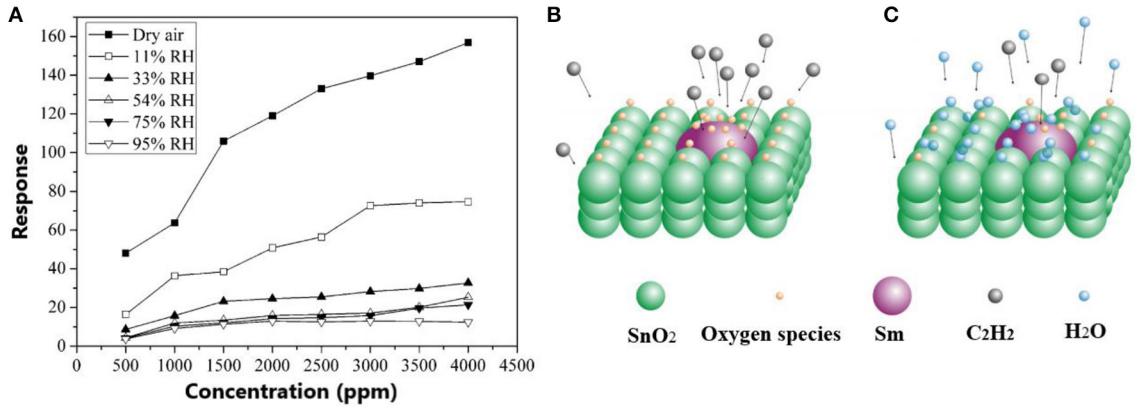

FIGURE 3 | (A) Sensor response of the Sm_2O_3-doped SnO_2 sensor to C2H2 at the different humidity content. **(B)** The gas sensing mechanism of Sm_2O_3-doped SnO_2 sensors to C_2H_2. **(C)** The gas sensing mechanism of Sm_2O_3-doped SnO_2 sensors to C_2H_2 in the humidity environment (reproduced from Qi et al., 2008).

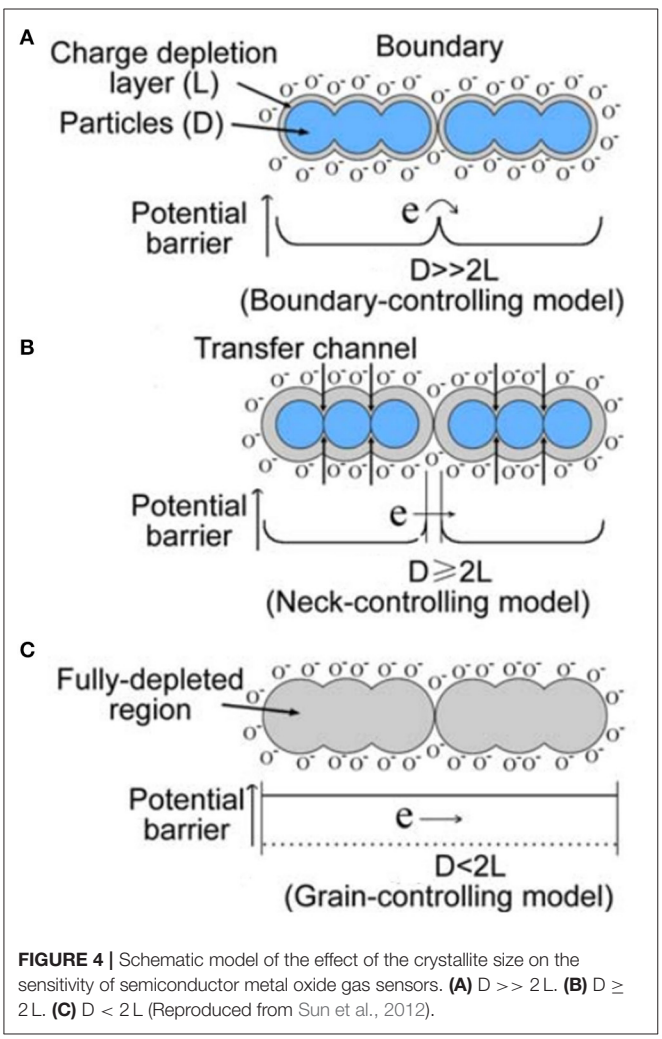

FIGURE 4 | Schematic model of the effect of the crystallite size on the sensitivity of semiconductor metal oxide gas sensors. **(A)** D >> 2 L. **(B)** D ≥ 2 L. **(C)** D < 2 L (Reproduced from Sun et al., 2012).

drastically. In such cases where D < 2L (**Figure 4C**), the grain size controls the sensitivity of the sensing material. These facts point out that not only the grain size but also the morphology and aspect ratio (D/L) of the grains in a gas sensing material plays a significant role in the characteristics of the gas sensors.

Moreover, another efficient way to modify the physical and chemical properties of SMOxs is their doping with other elements, especially those of redox capable cations. The crystal structure of the sensing material (e.g., tetragonal, cubic, or polymorphs anatase or rutile as in TiO_2) can be altered by the incorporation of elements into the crystal lattice through doping and thus the improvement of sensing, but in particular the selectivity of gas sensors. The introduced impurities and their levels change the original crystal parameters of SMOxs and simultaneously produce a large number of surface defects (dangling bonds) resulting in grain size reduction, increase of surface-active sites and in more conducive surfaces to enable gas adsorption and reaction (Li et al., 2013).

Effect of Morphology and Nanostructuring

In recent years, SnO_2 and TiO_2 nanostructures of various morphology, in particular 0D, 1D, and hierarchical 3D structures, were successfully synthesized, and it was demonstrated that morphology causes unique properties of the material, which is crucial for their further application.

The morphology and structure of MOx material that strongly affect the gas sensing properties are mostly controlled by the synthesis method. The selection of the synthesis method is decisive to achieve the desired grade of nanostructuring regarding morphology, grain/particle size, and the crystal and electronic structures of the sensing materials. The methods that are typically applied for the synthesis of the nanostructured SMOxs are electrochemical anodization (Gönüllü et al., 2012), hydrothermal method (Viet et al., 2015), template-assisted synthesis (Xu and Gao, 2012; Li Y.-X. et al., 2016), electrospinning (Osnat and Avner, 2015), and matrix-assisted pulsed laser evaporation (Caricato et al., 2011).

One-Dimensional SnO_2 Nanostructures

One-dimensional tin (IV) oxide materials provide high values of the specific surface while maintaining sufficient chemical

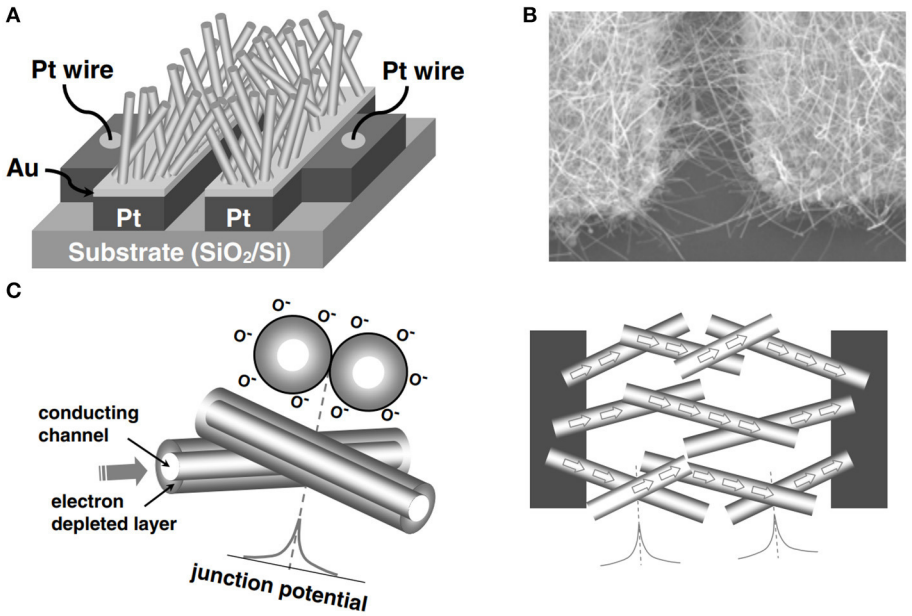

FIGURE 5 | (A) The schematic illustration for a network of SnO_2 nanowires floating above the SiO_2/Si substrate. **(B)** A SEM image of SnO_2 nanowires, selectively grown on the Au layer. **(C)** Schematic illustration of the gas sensing mechanism of the network-structured gas sensor (Reproduced from Choi et al., 2008).

and thermal stability with minimal energy consumption and low weight that make them the ideal substrates for gas sensing applications. Besides a specific surface area, the exposed crystal plane causes the great effect on the sensing characteristics. For instance, it was demonstrated that among four different morphologies of SnO_2 NPs, nanorods show excellent sensitivity and quick response due to the exposing of (111) planes (Hamanaka et al., 2016).

The most common methods of obtaining 1D SnO_2 nanostructures reported in the literature include the solvo/hydrothermal synthesis (Hien et al., 2011; Tan et al., 2011; Sial et al., 2017), chemical vapor deposition (Müller et al., 2012; Sayago et al., 2015; Stuckert et al., 2016; Shaposhnik et al., 2019), thermal evaporation (Shen et al., 2009; Thong et al., 2010; El-Maghraby et al., 2013), and sol–gel method (Li et al., 2017).

Moreover, to obtain 1D SnO_2 nanostructures, other synthesis approaches can also be used. Thus, Choi et al. (2008) showed that sensor based on SnO_2 NWs with self-assembled electrical contacts exhibit higher sensitivity to NO_2 compared to SnO_2 powder-based thin films, SnO_2 coating on carbon NTs (CNTs), or single/multiple SnO_2 nanobelts. The NW-based SnO_2 sensor was fabricated by a simple thermal evaporation method of metal Sn powder. **Figure 5A** shows the schematic illustration of SnO_2 NWs growing above the SiO_2/Si substrate bridging the gap between Au catalysts. **Figure 5B** presents the SEM image of the synthesized SnO_2 NWs from which it can be seen that NWs were selectively grown on the Au layer. Based on the obtained results, authors proposed the sensing mechanism of the network-structured gas sensor (**Figure 5C**) according to which the enhanced sensitivity of the created sensor can be attributed to the resistance changes due to both a potential barrier at NW/NW junctions and a surface depletion region of each NW.

Zhu et al. (2010) reported a good gas sensitivity and an excellent selectivity to acetone with rapid response and recovery times of 1D SnO_2 nanostructures, produced by the sonochemical method using the cotton fiber templates. In comparison to other techniques, the sonochemical method is an effective and efficient method regarding the response and recovery times, and the produce quantity enabling the synthesis of novel materials with unique properties.

The application of different synthesis approaches allows to vary not only the size and crystallinity of the particles but also the morphological possibilities to obtain tin (IV) oxide NWs (Shen et al., 2009; Thong et al., 2010; Müller et al., 2012), NTs (Lai M. et al., 2009; Lai Y. et al., 2009; Shi et al., 2010; Sadeghzade-Attar, 2019), nanorods (Wang Y.-L. et al., 2010; Hien et al., 2011), nanoribbons (Dai et al., 2002; Kong and Li, 2005; Pan et al., 2012), and nanobrushes (Stuckert et al., 2016). **Figure 6** shows examples of the SEM images of different 1D morphologies of SnO_2 nanostructures.

Sensor devices based on 1D SnO_2 nanostructures are capable to detect different gases and vapors including ethanol (Shen et al., 2012; Li T. et al., 2016), methanol (Shehzad et al., 2018), NO_2 (Law et al., 2002), CO (Qian et al., 2006; Shehzad et al., 2018), H_2S (Kumar et al., 2009), and CH_4 (Shehzad et al., 2018). **Table 1** presents the information on semiconductor gas sensors based on tin (IV) oxide nanostructures.

Nanotubular TiO_2 Surfaces or Layers

Use of 1D TiO_2 nanostructures for chemical sensing is recently summarized in the review article of Kaur et al. (2020). In this

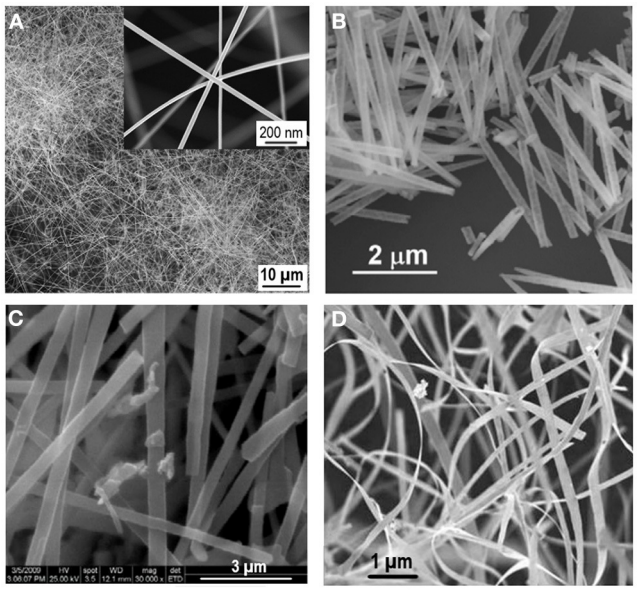

FIGURE 6 | SEM images of the 1D morphologies of SnO_2 nanostructures: **(A)** nanowires (reproduced from Shen et al., 2009). **(B)** nanotubes (reproduced from Lai M. et al., 2009). **(C)** nanorods (reproduced from Khuc et al., 2010). **(D)** nanoribbons (reproduced from Zou et al., 2011).

context, we concentrated solely on the previous studies related to gas sensing with nanotubular TiO_2.

Relying on the strong shape- and size-dependent conductivity changes observed in nanostructured MOxs, the spectacular surface modification of titanium foils yielding nanotubular TiO_2 layers is utilized by the gas sensing research community for the fabrication of high-performance gas sensing devices. Due to their unique physical and chemical properties, these nanostructured titania with different tubular shapes have been considered as one of the most promising materials (**Figure 7**). The results gained from the related studies until 2013 have been presented in the review article of Galstyan et al. (2013), revealing that the chemical sensor devices manufactured through integration of titania NTs are capable of responding in a variety of gases, such as hydrogen (Lee et al., 2011), ethanol (Galstyan et al., 2011, 2012b; Kilinc et al., 2011; Kwon et al., 2012; Perillo and Rodriguez, 2012), ammonia (Perillo and Rodriguez, 2012), and carbon monoxide (Galstyan et al., 2011; Lee et al., 2011) in dry and humid air environment and nitrogen dioxide in argon atmosphere (Gönüllü et al., 2012) (**Figure 8**). **Table 2** gives the details on some sensors that used TiO_2 NTs as gas sensing material.

Moreover, Lin et al. (2011) used sensor prepared with 400°C annealed TiO_2 NT array for formaldehyde sensing and reported the best response and good selectivity to formaldehyde concentrations from 10 to 50 ppm over 50 ppm methanol and 1,000 ppm ammonia in humidified air at room temperature. The authors point out that TiO_2 NTs act as p-type semiconductor due to the generation of electronic holes through the substitution of Ti sites with induced trivalent Fe when stainless steel is used as the cathode material as indicated by Allam and Grimes (2008).

Literature on nanotubular TiO_2 shows the employment of different synthesis approaches varying from electrochemical anodization (Gong et al., 2001; Beranek et al., 2003; Lai Y. et al., 2009; Galstyan et al., 2011), atomic layer deposition (ALD) (Foong et al., 2010; Chang et al., 2012; Huang et al., 2012), and hydrothermal synthesis (Suzuki and Yoshikawa, 2004; Choi M. G. et al., 2010; Zhao et al., 2012), among which the direct anodization of titanium foils appears to be the simplest route that yield the best promising gas sensing results.

The preparation of TiO_2 NTs by means of ALD requires the use of porous templates, such as high quality, nanoporous anodic aluminum oxide. The template-assisted technique carries various limitations, such as choice of substrate and post-processing separation from the template and the damage of tubes and other problems related to their transfer and applications onto the final substrates (Foong et al., 2010). The hydrothermal synthesis uses the solutions of anatase- and rutile-phased titania powders as precursors and for their postgrowth annealing. The electrochemical anodization refers to the anodic formation of titania NTs in a two-electrode system by oxidation and etching of metallic titanium in suitable electrolytes by variation of the anodization parameters, such as potential. The method allows direct growth of well-aligned and highly ordered TiO_2 tubular structures as thick continuous layers (see **Figure 9**) and the modification of the surface structure of titania at room temperature (Gong et al., 2001; Allam and Grimes, 2008; Galstyan et al., 2012b; Gönüllü et al., 2012).

Galstyan et al. (2011) produced transducer type of sensors by integrating titania NT arrays prepared by the direct anodization into the titanium thin films that are deposited on alumina transducers and contacted with the sputtered platinum interdigital electrodes. The results showed good sensing performances toward carbon monoxide and ethanol at 200°C using humid synthetic air as gas carrier.

Although most of the published research works concern NT arrays, there has been efforts to manufacture a single NT-based device by transferring the single TiO_2 NT onto a silicon wafer and integrating this into a field effect transistor (Liang et al., 2012).

From the synthesis method, it is reported that the post-annealing temperature of TiO_2 NTs influences the sensitivity and gas sensing behavior of the sensors, mainly because of variation of TiO_2 phase constituents and also due to the differences in surface area, grain size, and surface chemistry (Lin et al., 2011; Gönüllü et al., 2012). Gönüllü et al. (2012) reported that the nanotubular TiO_2 layer annealed at 450°C consists of only anatase phase, and the produced sensor detects NO_2 selectively at a concentration range varying from 10 to 100 ppm and gas temperatures from 300 to 500°C, whereas the loss of sensitivity toward NO_2 on annealing the nanotubular TiO_2 layer at 700°C is anticipated to be due to the formation of some rutile phase.

The published research works on nanotubular TiO_2-based gas sensors revealed that on the one hand a high surface area for the gas absorption and accessible open space and gaps for the surface/gas interaction exhibit high sensitivity toward a variety of oxidizing and reducing gases; on the other hand, their selectivity appears to be influenced factors other than the structuring and size. One indication is made regarding the grade of the sensitivity

TABLE 1 | List of selected sensors prepared using one-dimensional SnO_2.

Preparation method	Dopant	Contacts	Carrier gas	Measurement	Test gas	Detection limit	Sensitivity	Response/ Recovery times	References
Thermal evaporation	La_2O_3	Au	Air	Dynamic flow	Ethanol Acetone	10–100 ppm 100 ppm	57.3 (at 100 ppm) 34.9 (at 100 ppm)	1 s/110 s 1 s/178 s	Hieu et al., 2008
Thermal evaporation	Pd	Pt	Air	Dynamic flow	H_2	100–1,000 ppm	253 (at 1,000 ppm)	–/–	Shen et al., 2009
Sonochemical	None	Pt	Air	Static	Acetone	20 ppm	6.4	10 s/9 s	Zhu et al., 2010
Electrospinning/ Atomic layer deposition	None	Pt	Air	Dynamic flow	Ethanol H_2, CO, NH_3, NO_2	5–100 ppm 100 ppm	188 (at 100 ppm) –	< 5 s/– –/–	Kim et al., 2010
Hydrothermal	Zn	Au	Air	Static	Methanol	1–100 ppm	59 (at 50 ppm)	–/–	Ding et al., 2010
Template	none	Pt	N_2	Dynamic flow	Methane	125–2,500 ppm	–	–/–	Biaggi-Labiosa et al., 2012
Thermal evaporation	ZnO	Au	Air	Dynamic flow	NO_2	1–5 ppm	619 (at 5 ppm)	–/–	Park et al., 2013
Thermal evaporation	None	Pt	Air	Dynamic flow	H_2	100–1,000 ppm	5.5 (at 1,000 ppm)	–/–	Shen et al., 2015
Sol-gel	None		Air	Dynamic flow	Ethanol	1–500 ppm	∼6.2 (at 100 ppm)	18 s/27 s	Li et al., 2017
Electrospinning	PdO-ZnO	Au	Air	Static	Acetone	1 ppm	5.06	20 s/64 s	Koo et al., 2017
Carbothermal reduction of SnO_2 and graphite powders	None	Au	Air	Dynamic flow	CO Methane Methanol	20 ppm 400 ppm 50 ppm	3.2 1.2 6.65	57 s/91 s 70 s/70 s 32 s/108 s	Shehzad et al., 2018
CVD	Carbon	Silver paste	N_2	Dynamic flow	Ethanol Acetone CO H_2 Toluene NH_3	1–50 ppm	∼4.2 ∼3.3 ∼2.1 ∼2.3 ∼2.1 ∼1.3	–/–	Tonezzer et al., 2019

and selectivity change from reducing to oxidizing gases through the variation of post-annealing temperatures applied to the NTs prior to the gas exposure, emphasizing the importance of state of phases (Gönüllü et al., 2012). The other indication is that the effect of cation contamination and dopants on the sensor behavior (n-type vs. p-type) and the selectivity of the sensors toward a specific gas. The effect of contaminant trivalent Fe is mentioned in Lin et al. (2011) to improve the selectivity of the sensors toward room temperature detection of formaldehyde.

Investigations that are performed to demonstrate the role of niobium doping on titania NT conductance and gas sensing property displayed that though the conductance remained below the standard electronics, a remarkable sensing performance change is observed with the presence of 0.14 at% Nb dopant in TiO_2 NTs (Galstyan et al., 2012b; Liu et al., 2012). The achievement of Nb doping was enabled by the anodization of Nb–Ti thin films. Liu et al. (2012) indicate that the presence of 5 wt.% Nb is required as dopant in TiO_2 NTs for the obtainment of sufficiently high conductance (e.g., 10^{-4} S) as maintaining good hydrogen sensing performances.

Bayata et al. (2014) have demonstrated that the 9–10 at.% Al doping of TiO_2 NTs can be achieved by parameter optimized anodization of the 5-μm thick TiAl thin films grown by the cathodic arc physical vapor deposition (CAPVD) method. In order to avoid any short circuits between the Pt pads used for contacting the sensors and any residue metallic layer, the TiAl metallic films on alumina were totally anodized in ammonium fluoride (NH_4F) containing ethylene glycol (EG) electrolyte. The anodized TiAl nanopore structures were then subjected to the heat treatment at 485°C for 3 h to obtain anatase phase, and the sensors prepared with Pt pads tested for the hydrogen sensing performance in the range of 50–2,500 ppm hydrogen at different temperatures (25–350°C). Doping of titania NTs with aluminium resulted in a decrease of resistance and yielded, already at room temperature, high sensitivity and quick response

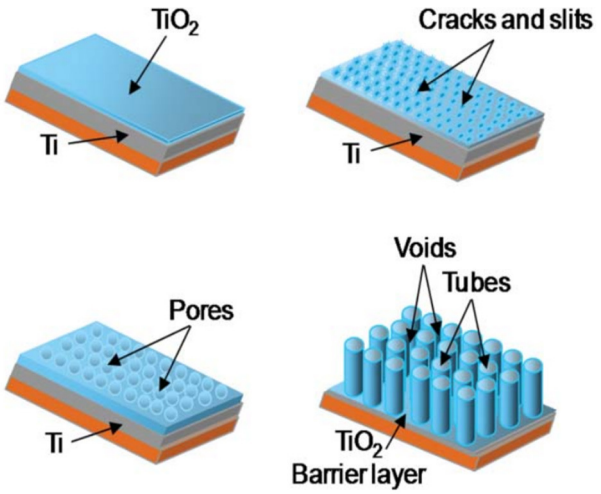

FIGURE 7 | Schematic of the evaluation of TiO_2 nanotube arrays by means of potentiometric mode anodization (Reproduced from Galstyan et al., 2011).

toward H2. This sensitivity increases with the increasing of operating temperature.

Lai and Sreekantan (2013) reported another interesting approach to prepare mixed TiO_2 NTs by incorporating WO_3 throughout the TiO_2 NT walls by a wet impregnation method. An anodized TiO_2 NT foil was dipped into an ammonium paratungstate (APT) aqueous solution with different molarities for 1 h. To decompose the APT into WO_3, a final annealing is applied at 400°C. These WO_3-TiO_2 NTs employed as photoelectrochemical catalysts.

In a similar approach, Gönüllü et al. (2015) have introduced trivalent Cr into the TiO_2 NTs to obtain selective nitrogen dioxide gas sensors displaying p-type semiconducting sensing behavior. Response and recovery times of the sensors from Cr-doped TiO_2 NTs were faster and yielded better signal quality as opposed to the slow and drifty signal of those sensors manufactured with the undoped TiO_2 NTs. The authors have reported that 2.5% Cr doping of TiO_2 NTs results in the improvement of the high-temperature NO_2-sensing capability, especially in the temperature range of 300–500°C and in the gas concentrations between 25 and 100 ppm. Furthermore, it was observed that the Cr doping reduces the response toward CO drastically, whereas the response toward NO_2 increases demonstrating the decrease of cross-sensitivity almost to a negligible level under mixed gas detection of NO_2, probably due to the alteration of the band gap through the conductor change from n-type to p-type (**Figure 10**).

Ni-doped TiO_2 NTs synthesized by the anodization of NiTi plates with nominal composition of 50.8 at% Ni under 20 V in a non-aqueous electrolyte of 5% EG/glycerol containing 0.15 M $(NH_4)_2SO_4$ and 0.2 M NH_4F (Li et al., 2013) exhibited good response and high sensitivity to an atmosphere of 1,000 ppm hydrogen at both room temperature and at temperatures up to 200°C.

Tong et al. (2019) gas synthesized a cobalt-doped free-standing TiO_2 NTs (Co-doped TiNT) array film by a one-step anodization followed by the immersion method. The resulting sensor yields superior selectivity, stability, and reproducible sensor response value at 199.16 for 50 ppm H_2S, indicating an improvement by 7.6 times higher than undoped ones.

This large number of previous works points out excellently the potential of the nanostructured and nanotubular SMOxs for the use in gas sensors to achieve high sensitivity and selectivity. The implementation of these ideas to the commercialized gas sensors however stumbles in the technological barriers and requires industrial acceptance of nanotechnological processing in the production lines.

Surface Loading and Bulk Doping

High selectivity of the created sensors to the detected gases can also be provided by the surface modification and doping of SnO_2 and TiO_2 nanostructures with catalytic additives or other oxides.

Nobel Metal Surface Loading

The NMs, such as Ag, Au, Pd, Pt, and Rh NPs loaded/decorated onto the surfaces of semiconducting SnO_2 and TiO_2 enhance the gas sensing performance, due to the creation of new active centers on the MOx surface or changing the electronic structure of material (Epifani et al., 2012). As the alteration of electronic structure changes the electron accumulation due to the different work functions between NMs and semiconducting oxide (Chen et al., 2017), the chemical sensitization relies on effective catalytic properties of NMs (Xing et al., 2018).

The electron transfer between the NM particles and MOx surface and the electron depletion layer formation on their surface increase the resistance and make them sensitive to the resistance changes on contact with the reducing gas molecules. In such case, the adsorbed oxygen species (O^{2-}, O^{-}, and O^{2-}) on the NM decorated surface of MOx lead to an obvious change in resistance (David et al., 2020). The loading of NMs onto MOx surfaces increases the capacity for adsorbing oxygen molecules, which simultaneously can accelerate the reaction between adsorbed oxygen species and reducing gas molecules. On interaction with reducing gas molecules, first their adsorption on the NM surfaces occurs, which is then followed by redox reactions with the adsorbed oxygen species to promote the sensing response.

In the case of the metal loading, sensing mechanism can be explained by the formation of nano-Schottky barrier between the metal NP/nanocluster and surfaces of semiconductor. Due to the metal/semiconductor contact, the electron transfer occurs, forming an area with high resistance (the barrier layer) around metal NP. Thus, metal NP/nanocluster represents an electronegative surface. Under the gas/vapor exposure, the area with high resistance transforms to the area with high conductance, this brings about the great enhancement of the sensing performance. Namely, metal-decorated semiconductors exhibit higher sensitivity and selectivity, lower working temperature, shorter response/recovery time, and better reproducibility (Wang et al., 2012).

Figure 11 presents the schematic diagram for the sensing mechanism of sensor based on Pd-doped TiO_2 NPs. As one can see, at the certain temperature, oxygen ions with different valence

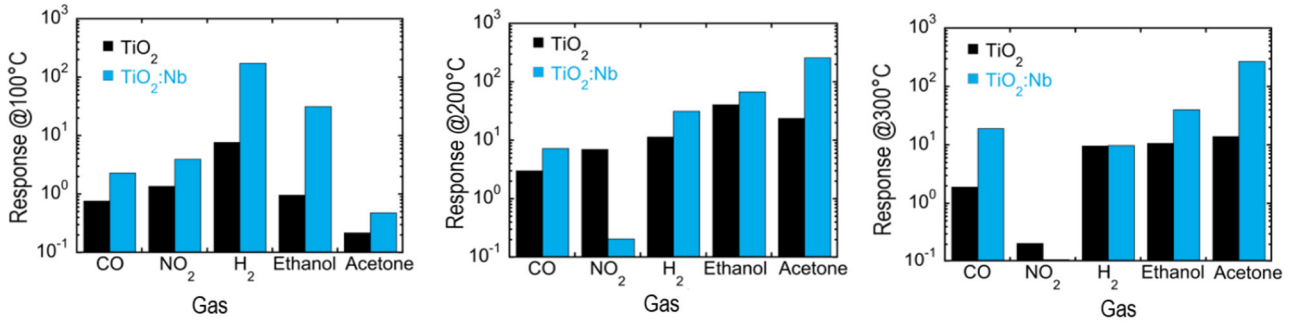

FIGURE 8 | Demonstrating the response improvement of gas sensors prepared with nanotubular TiO_2 sensing layers (blue columns) in comparison to those with bulk TiO_2 (black columns) toward CO, NO_2, H_2, Ethanol, and acetone at 500, 10, 1,000, 500 ppm, respectively, and working temperatures 100, 200, and 300°C (Reproduced from Galstyan et al., 2012a).

states are formed, and electron is excited and captured by the oxygen adsorbed on the TiO_2 surface functionalized with Pd. This results in the electron depletion and large base line resistance of the sensing material. Upon the gas exposure (e.g., butane), the electrons are released back to the sensing material, leading to the thinner space–charge layer and resistance decreasing. In this case, the enhancement of sensing performance can be explained by the metal–semiconductor contact formation between Pd and TiO_2 as shown in **Figure 11**. When TiO_2 contact with Pd NPs, the electrons transfer from TiO_2 to Pd NPs and accumulate on its surface. Electron-rich Pd NPs provide more sites for oxygen species adsorption on the sensitive layer surface, resulting in a significant increase of sensor response (Chen et al., 2017).

Thus, for instance Ag-decorated tin (IV) oxide nanorods, obtained using microwave-assisted green synthesis, exhibit twice as much response and almost twice reduced response/recovery time to ethanol (Zhang et al., 2017). The modification of SnO_2 NPs with Au allows to reduce response time of gas sensor to hydrogen (Yin et al., 2019). Ag-modified TiO_2 porous NPs synthesized by one-pot hydrothermal method results in sensors yielding good selectivity (SF $\sim$ 12.6) toward 100 ppm acetone against other volatile organic compounds (VOCs) (Wang et al., 2020).

Yang et al. (2019) have synthesized 1D core–shell structures based on the coating of silver NWs (Ag NWs) with a layer of TiO_2 NPs where the length of the Ag NWs were $\sim$10 μm and the diameter around 100 nm as the TiO_2 polycrystalline shell was 10–15 nm in thickness. These Ag NWs at TiO_2 core–shell nanocomposites exhibited better sensing properties relying on the Schottky barrier that exists at the interface between the Ag NWs and the TiO_2.

One of the effective ways to improve the gas sensing performance is the formation of the metal/MOx nanoclusters, which are characterized by large surface-to-volume ratios, selective and rapid response to different gases (Ayesh, 2016). Nanoclusters of Au, Pd, and Pt are widely used to enhance the sensitivity and selectivity of the MOx sensors. For instance, in the review article on the gas sensors modified with gold NPs, it was shown that the functionalization of MOx surfaces with gold nanoclusters can be used for the development of high-performance gas sensors (Korotcenkov et al., 2016). Rane et al. (2015) prepared SnO_2 thin films covered with a platinum layer of 80 nm thickness and showed that Pt–SnO_2 composite exhibits promoted sensing properties for the H_2 detection at low concentration (150 ppm). The Pt modification allowed the decreases in sensor operating temperature and response/recovery times to 0.5 and 25.5 s, respectively. Authors concluded that in this case, Pt acts as a promoter for hydrogen molecules dissociating at low temperatures and activator for the surface reactions between oxygen species and adsorbed hydrogen.

Bulk Integration of Dopants

Among resistive sensors, SMOxs are attracting more attention as gas sensing materials due to their simple working principle, yielding high sensitivity, and being lightweight and low cost. Although this type of sensors presents many advantages, its selectivity, stability, and sensitivity need to be tuning for the practical applications. Many researchers have suggested various ways to tune these sensing characteristics, which include the use of specific filters like zeolite thin films, the addition of noble catalytic metals to promote the reaction to specific gases, the use of composite MOxs, and the use of dopants.

Doping of an MOx has proven to be a facile and suitable approach to overcome the drawbacks of pristine SMOx gas sensing materials. The presence of dopants can cause the formation of new acceptor or donor states, shifting the bulk or surface Fermi level and changes the original crystal parameters of the SMOx. Tong et al. (2019) has proven by density functional theory (DFT) calculation that the doping method can remove the electrons from the top of the valence band, or injection the electrons at the bottom of the conduction band, thus reducing the forbidden band width of the semiconductor materials to improve the gas sensing performances. Up to date, many metallic dopants have been integrated to TiO_2 (Al, Cr, Nb, Co, Zr, Mn, Ni, Cu, Ta, W, Fe, and Y) to yield sensors with enhanced gas sensing properties, relying on hinderance or promotion of phase transformation, change in surface potential, increase of chemical

TABLE 2 | List of selected sensors prepared using nanotubular TiO_2.

Preparation method	Dopant	Contacts	Carrier gas	Measurement	Test gas	Detection limit	Sensitivity	Response/ Recovery times	References
Ti foil anodization	None	Pt	N_2	Dynamic flow	O_2	1,2–4%	∼168 (at 4%)	–/–	Lu et al., 2008
Ti foil anodization	None	Pt	N_2	Dynamic flow	H_2	100–5,000 ppm	20 (at 1,000 ppm)	–/–	Sennik et al., 2010
Ti film on alumina anodization	None	Pt	Air	Dynamic flow	CO Ethanol	500 ppm 500 ppm	1,400 80	<1 min/– <1 min/–	Galstyan et al., 2011
Ti foil anodization	None	Stainless steel	Air	Static	Ethanol NH_3	400 ppm 150 ppm	– –	–/– –/–	Perillo and Rodriguez, 2012
Ti thin fil anodization	None	Sputtered Au	Dry air	Dynamic	VOC	5,000 ppm	2–37	–/–	Kilinc et al., 2011
Ti foil anodization	None	Sputtered Pt	Ar	Dynamic air	NO_2 CO	10–100 ppm 25–75 ppm	∼5 (at 50 ppm) ∼2.6 (at 50 ppm)	3–4 min –/–	Gönüllü et al., 2012
TiO_2 nanotube Anodization of $Ti_{35}Nb$ alloy	Nb-doped	Pt electrodes connected to the Cu pads of PCB	Air and N_2	Static	H_2	50 ppm-2%	∼5 (at 1000 ppm)	100 s/–	Liu et al., 2012
TiAl arc-PVD deposited thin films	Al-doped	Sputtered Pt	Dry argon	Static	H_2	50–2,500 ppm	255 (at 1,000 ppm)	33 s/5 s	Bayata et al., 2014
Ti foils Anodization of	Cr-doping by chemical immersion	Sputtered Pt	Ar	Dynamic air	NO_2	25–100 ppm	∼3.5 (at 100 ppm)	3-6 min	Gönüllü et al., 2015
TiO_2 nanotube Electrochemical anodization	Ni-doped	Sputtered circular Pt	N_2	Dynamic	H_2	50 ppm-2%	∼40 (at 1,000 ppm)	–/–	Li et al., 2014
Ti one step anodization	Co-doped by immersion in Co-chloride		50% humidity	Static	H_2S	1-50 ppm	26.2 (at 50 ppm)	22 s/6 s	Tong et al., 2017

activity, charge carrier concentration and the amount of adsorbed oxygen ions and altering of the band gap.

The structures of SMOx and added metal compounds can be presented by the Me ions incorporated in the MOx lattice, clusters on the surface, or ordered mixture of different MOx materials. **Figure 12** shows different structures on MOx materials and added metal or MOxs.

One of the early studies on Cr doping is given by Ruiz et al. (2003) for NO_2 sensing that suggests a tendency for the electronic conduction to alter from n- to p-type as proven by a shift of the binding energy (BE) at the band edge to the lower energy side with Cr contents increasing to 20 at.%. Other following works with the trivalent Cr-doped TiO_2 have proven the potential of chromium in gas sensing (Lyson-Sypien et al., 2012). Later, Gönüllü et al. (2015) have reported that as small as 2.5% Cr doping of TiO_2 NTs was sufficient to improve the NO_2-sensing capability (25 and 100 ppm) under high-temperature flowing gas in the range of 300–500°C.

Al–Co doping of sputtered synthesized TiO_2 layers also yield sensors that can detect 50–200 ppm NO_2 under humid hot gas exposure between 400 and 800°C and exhibit an altered semiconductor behavior from the p- to n-type in the temperature range of 600 and 800°C (Saruhan et al., 2013). Li et al. (2013) have also demonstrated p-type hydrogen sensing with Al and V doping of TiO_2.

Substitution of Ti by Ni by different synthesis methods such as anodization (Li et al., 2013) and wet chemical synthesis of particles (Lontio Fomekong et al., 2020) resulted in change in the conductivity type, inducing effective reduction in the band gap of anatase phase, and thus playing a great role in sensing properties. The presence of Ni as an impurity in the TiO_2 lattice is also known to create more oxygen vacancies due to the introduction of higher impurity levels that directly affect the gas sensing performance (Sun et al., 2012; Postica et al., 2018; Degler et al., 2019).

Lontio Fomekong et al. (2020) have recently synthesized Ni-doped TiO_2 NPs by the oxalate-assisted coprecipitation method and conducted research to analyze the effect of Ni dopant on gas sensing properties. Their results indicate that the Ni doping modifies the ratio between the anatase and rutile phases that has proven to have an impact on the hydrogen sensing properties. Best H_2 sensor response rate (DR/R0 = 72%) and selectivity were obtained with 0.5% Ni-doped TiO_2, exhibiting almost equal amounts of anatase and rutile. The significant improvement

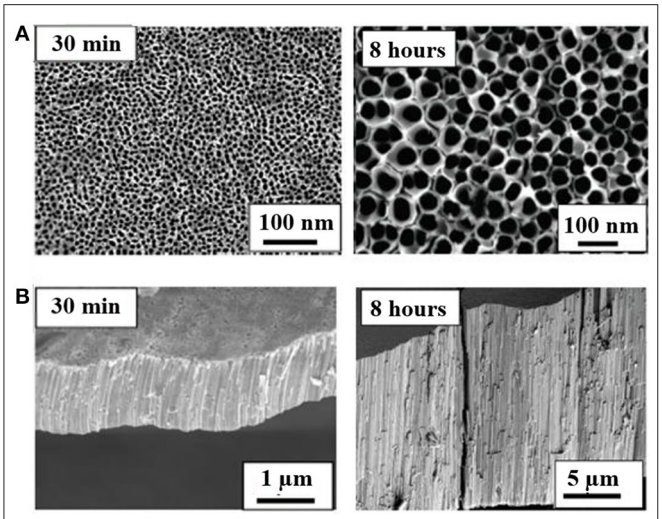

FIGURE 9 | Top-view **(A)** and cross-sectional **(B)** SEM micrographs of undoped TiO_2 NTs synthesized by direct anodization in Ethylene Glycol (EG) based solution under an applied voltage of 60 V for different anodization times (Reproduced from Gönüllü et al., 2014).

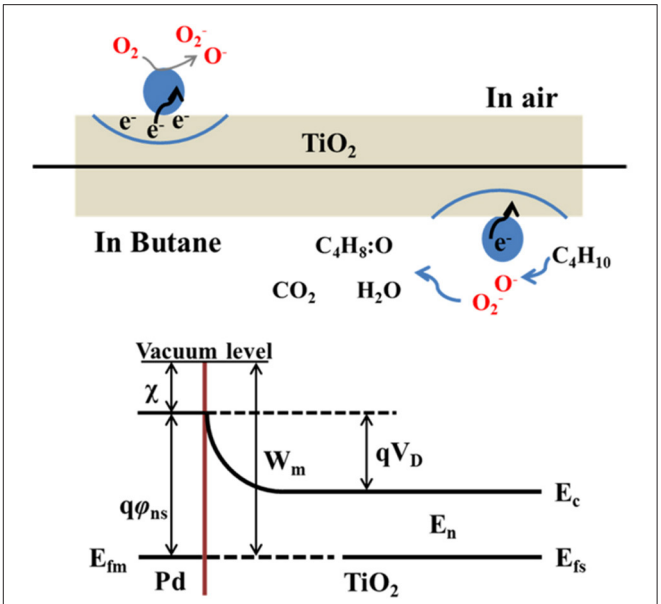

FIGURE 11 | A schematic diagram of Pd-doped TiO_2 nanoparticles based sensor for enhancement caused by metal-semiconducor. Pd nanoparticles showed in blue (Reproduced from Chen et al., 2017).

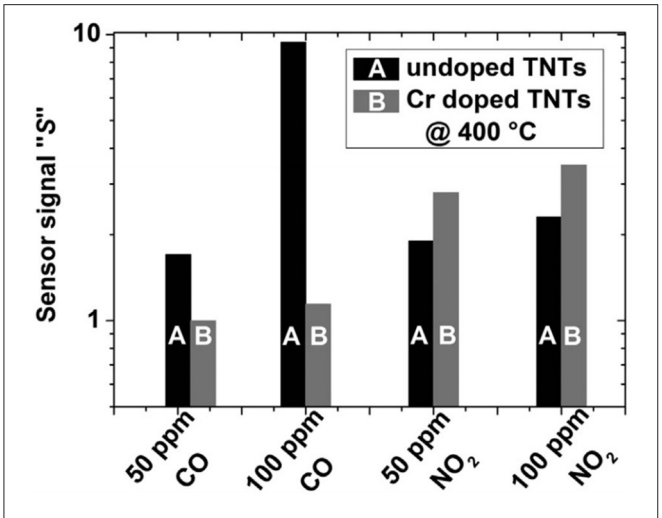

FIGURE 10 | Comparison of sensor signal obtained with undoped and Cr-doped TiO_2 nanotubes toward 50 and 100 ppm CO and NO_2 under single gas exposure at 400°C (Reproduction from Gönüllü et al., 2015).

of the sensing performance with 0.5% Ni-doped TiO_2 NPs is mainly attributed to the formation of the highest number of n–n junctions present between anatase and rutile that influence the quantity of adsorbed oxygen (i.e., the active reaction site) on the surface and the conductivity of the sensing material.

By means of the same synthesis method, Lontio Fomekong et al. (2019) have synthesized Co-doped TiO_2 and demonstrated that the main phase is anatase at the doping level lower than 1 mol% Co and rutile at the doping level equal or higher than 1 mol%. Accordingly, the sensors also show different properties as the Co-dopant concentrations alters. The TiO_2 NP sensors with lower Co-dopant yield similar to the undoped TiO_2, n-type behavior and significant H_2 selectivity as those doped with higher Co-concentrations exhibit p-type behavior and higher selectivity to NO_2 at 600°C.

Liu et al. (2015) prepared W-doped TiO_2 NPs by a non-aqueous sol–gel route and obtained gas sensors with a low detection limit, good linear dependence, good repeatability, and long-term stability toward butane. It is reported that the response to 3,000 ppm butane increases from 6 to 17.8 through the doping with 5% tungsten, and at the same time, the recorded response and recovery times were as fast as 2 and 12 s, respectively.

Zhang et al. (2019b) synthesized nanoporous Sn-doped TiO_2 NPs by hydrothermal method that yield sensors exhibiting good response, linear correlation, repeatability, and long-term stability toward VOCs at the operating temperature of 240°C. In particular, the 2.5% Sn-doped TiO_2 NPs show a high gas response, the highest response being toward 100 ppm VOCs (i.e., 21.19). These values demonstrate the potential application of Sn-doped TiO_2 NPs for the VOC detection.

The sol–gel technique was used to prepare Fe-doped TiO_2 thin films for CO sensing application. The gas sensing behavior of the films was studied by measuring the electrical resistance and by the exposure of different CO concentrations. It was observed that Fe doping of TiO_2 has a significant effect on the resistivity of the doped TiO_2 thin films. The sensors having 7% (weight/volume) Fe-doped TiO_2 exhibited high sensitivity and good response/recovery on exposing 100–900 ppm CO gas in Argon carrier gas (Kumar et al., 2015).

Nb doping of TiO_2 is also adopted for gas sensing applications (Sharma et al., 1996, 1998; Liu et al., 2012). The flame-made Nb-doped TiO_2 spherical NPs with crystallite sizes in the range of

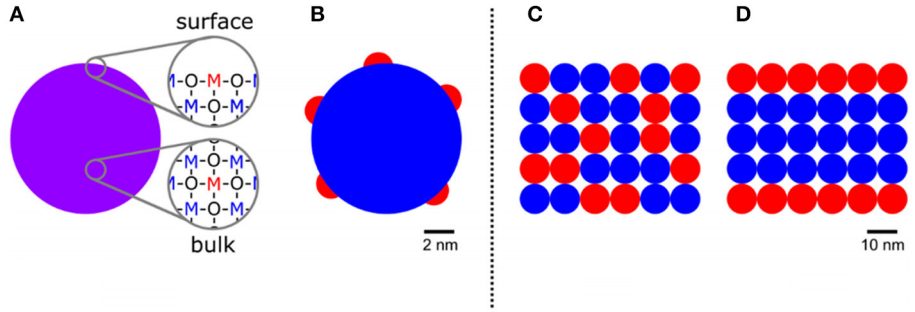

FIGURE 12 | Different structures of MOx (blue) and added metal/metal oxide (red). **(A)** Additives incorporated in the MOx lattice at the surface/in the bulk. **(B)** Additives forming a separate phase located on the MOx surface. **(C)** Random arrangement of MOx and additive grain. **(D)** Ordered arrangement of MOx and additive grain (Reproduced from Degler et al., 2019).

10–20 nm employed to prepare sensing films by the spin coating technique. The gas sensing of acetone (25–400 ppm) studied at operating temperatures ranging from 300 to 400°C in dry air, whereas the gas sensing of ethanol (50–1,000 ppm) at operating temperatures ranging from 250 to 400°C in dry air. About 3 at.% Nb dispersed on TiO_2 sensing films yield relatively high sensor response in comparison to those that were produced from undoped TiO_2 (Phanichphant et al., 2011).

Bao et al. (2019) have synthesized Nb-doped rutile/anatase TiO_2 heterophase junction thin films through one-step hydrothermal self-adjusted Nb doping for a highly sensitive H_2 sensor. The H_2 concentration detection range is remarkably expanded from 1 to 12,000 ppm for nanorod-decorated film as a result of the massive accumulation of reactive pre-absorbed on the surface due to the Nb doping. The H_2 response at 1 ppm is recorded as 22.5% and reaches 98.9% at 8,000 ppm H_2 for the bilayer structure.

Khatoon et al. (2020) investigated the Co and Ni doping of SnO_2 material with aim to develop multisensor array. **Figure 13** shows the selectivity radar chart of gas sensor array consisting of three different layers—pure SnO_2, Co-doped SnO_2, and Ni-doped. It may be noticed that metal loading of SnO_2 changes the selectivity of sensitive material. Thus, SnO_2 sensitive layer doped with Co exhibits higher selectivity to toluene, whereas Ni-doped SnO_2 has good sensor response to isopropyl alcohol and 1-propanol.

These studies reveal that the type of the metallic dopant has influence on the type of sensing gas. Trivalent gases, such as Al and Cr, yield better sensing and selectivity toward NO_2 at higher temperatures, whereas high valency dopants, such as Sn, W, and Nb, give sensors with good response toward reducing gases.

Composites and Heterostructures

It is known that semiconductor sensors based on a single MOx do not provide simultaneously an excellent comprehensive sensing performance on sensitivity, selectivity, and stability (Zhao et al., 2019). Among various approaches for improving the gas sensor performance, the formation of heterostructures between two semiconductors causes particular interest (Wang et al., 2018; Nakate et al., 2020). Heterojunction structures based on SnO_2, TiO_2, and other MOx materials characterize by outstanding gas sensing properties (Li et al., 2015). In comparison with single MOx materials, gas sensors fabricated based on p–n heterojunction structures exhibit high sensor response, lower working temperature, and short response time (Khoang et al., 2012; Shanmugasundaram et al., 2013). The improvement in conductivity and in response and recovery times in p–n junction structures related to the bending of conduction and valence bands and equalization of Fermi levels (Wang Z. et al., 2010; Shao et al., 2013).

In recent years, gas sensors based on SnO_2 and TiO_2 nanostructures with p–n and n–n heterojunctions have been developed. To produce composites and heterostructures, different synthesis approaches can be applied, including the hydrothermal method (Zeng et al., 2012; Shanmugasundaram et al., 2013; Li et al., 2015; Yang et al., 2015), electrospinning technique (Wang Z. et al., 2010), chemical vapor deposition process (Shao et al., 2013), sputtering techniques (Maziarz, 2019; Sharma et al., 2020), and flame spray method (Lyson-Sypien et al., 2017).

For instance, Li et al. (2015) created the SnO_2-SnO composite by hydrothermal method, which exhibit high selectivity to NO_2 with the detection limit and sensitivity of 0.1 ppm and 0.26 ppm^{-1}, respectively, at 50°C. Authors explained the improved sensor performance by the formation of p–n junction through the growth of SnO_2 nanocrystals on SnO nanoplates. Sharma et al. (2020) fabricated a highly sensitive and selective NO_2 gas sensor based on SnO_2/ZnO nanostructures. In this case, the established n–n heterojunctions between SnO_2 and ZnO significantly rise the electrical resistance, resulting in a high gas performance, in comparison with pure SnO_2 and ZnO materials. The created TiO_2-B_2O_3 composite gas sensor shows a good performance to low H_2 concentration at different operating temperatures. Moreover, the created gas sensor showed a good sensor performance at temperatures below 100°C (Chachuli et al., 2018).

Besides the usage of single SnO_2 and TiO_2 material for sensitive layers, the sensing characteristics can be improved by the creation of SnO_2/TiO_2 composites (Radecka et al., 2011; Maziarz, 2019). The combination of SnO_2 with TiO_2 leads to

the formation of n–n heterojunction, which can facilitate the electron transfer and promote oxygen pre-adsorption that effects on the improved sensing performance of the sensor devices (Zeng et al., 2012; Yang et al., 2015). For instance, it was found that TiO_2/SnO_2 composite sensing materials characterized by three times higher response to the triethylamine low concentration in comparison with TiO_2 sample (Jia et al., 2018). Kim and Choi (2017) in their work synthesized hybrid sensing material based on SnO_2 NPs and TiO_2 NTs with high sensitivity and short response time to CO and CH_4 gases. Lyson-Sypien et al. (2017) synthesized TiO_2/SnO_2 heterostructures with different SnO_2/TiO_2 ratio by the flame spray method. The study on sensing characteristics of the obtained materials showed the detection limit of TiO_2/SnO_2 heterostructures is lower than 1 ppm, especially in the case of SnO_2-rich samples. However, the response time for SnO_2-rich samples is much longer in comparison with TiO_2-rich materials.

The TiO_2-B_2O_3 composite gas sensor shows a good performance to low H_2 concentration at operating temperatures above 100°C (Chachuli et al., 2018). The Pt functionalization of 3D SnO_2 nanostructures results in the fast response/recovery speed, good reproducibility, and higher response of the modified structures in comparison with pure SnO_2 sensing material (Liu Y. et al., 2017).

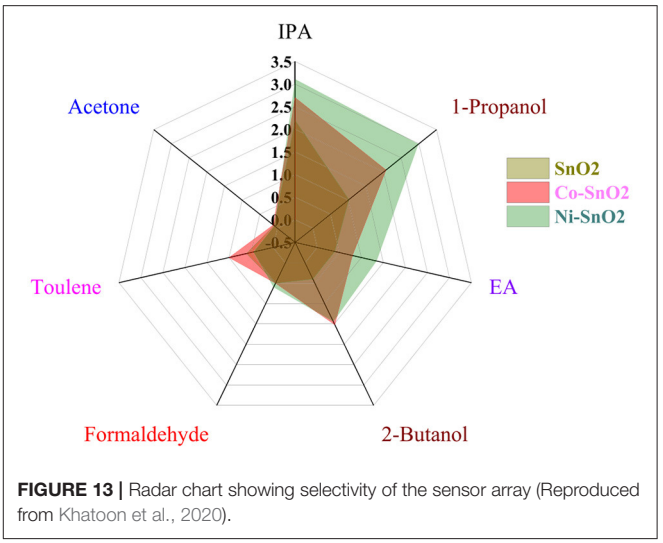

FIGURE 13 | Radar chart showing selectivity of the sensor array (Reproduced from Khatoon et al., 2020).

Core–Shell Nanostructures

Recently as an alternative for the increasing the response of MOx gas sensors, hollow, and core–shell structures were proposed. The core–shell structures are heterogeneous NPs comprise of two or more materials, wherein one nanomaterial forms the core at the center and the other material or materials act as the shell, located around the core. Thus, core–shell nanostructures belong to the biphasic systems with inner and outer parts made up of different materials. The core–shell nanostructures can be labeled as nanocomposites, but in comparison to the nanocomposites with uniform structure, core–shell NPs usually have the noticeable separation between core and shell (Khatami et al., 2018). Thereby the physical properties of the core and shell can be easily and separately adjusted, whereas the individual properties of core and shell nanostructures bring the unique properties of core–shell particles compared to one-component materials (Rai et al., 2015). These structures exhibit new functional materials with unique structure features, such as providing more active cites for the electrochemical interaction in comparison with solid nanostructures, which results in improved electronic and sensing properties (Majhi et al., 2018; Zhang et al., 2019a).

A variety of methods have been introduced for the synthesis of SnO_2 and TiO_2 core–shell nanostructures, having NMs (Au, Ag, Pt, and Pd) as a core and SMOxs (TiO_2 and SnO_2) as a shell, including the sol–gel synthesis (Sakai et al., 2006; Haldar and Patra, 2008; Angkaew and Limsuwan, 2012; Goebl et al., 2014; Kanda et al., 2014), aqueous chemical technique (Oldfield et al., 2000), intermetallic-based dry oxidation method (Yu et al., 2008), sonochemical technique (Tripathy et al., 2013), and hydrothermal method (Song et al., 2015).

Besides NMs, other MOxs (NiO and WO_3) are used for the SnO_2 and TiO_2 core–shell formation by the hydrothermal method (Zhang et al., 2014), sol–gel approach (Poloju et al., 2017), combination of hydrothermal and chemical bath deposition (Cai et al., 2013, 2014).

The core–shell structures have shown better sensing properties in comparison with pure MOx nanostructures and nanocomposites of MOxs with NMs. In this case, the MOx shell provides high thermal and chemical stability to NM. And as physical and chemical properties of core and shell can be varied separately, core–shell nanostructures are promising materials for high-performance sensing devices (Rai et al., 2015).

For instance, SnO_2 core–shell spheres, synthesized by the hydrothermal process, characterized by more active sites for gas molecule adsorption, and as a result, sensors based on them exhibit higher sensing response to the ethanol compared with pure SnO_2 particles (Zhang R. et al., 2019). Liu D. et al. (2017) showed that hybrid materials based on Ag NWs/TiO_2 array with core–shell nanostructure display ultrasensitivity to the CH_4 already at room temperature. The obtained material showed detection limit of 20 ppm, which is below the most existed CH_4 sensors. In their research, Raza et al. (2020) demonstrated great perspective of 1D core–shell heterostructures for the creation of high-performance gas sensors. SnO_2/NiO heterostructures, obtained by vapor–liquid–solid and atomic layer deposition techniques, showed excellent sensing properties to hydrogen due to the high surface area of 1D single-crystalline SnO_2-core NWs, the NiO–shell layer with an optimized thickness, formation of a p–n junction, and chemical sensitization of NiO to hydrogen.

Song et al. (2015) studied the influence of shell thickness on sensing characteristics of Au at SnO_2 core–shell nanostructures and found that the response for the CO detection was increased with the increasing shell thickness and showed the highest sensing response for 15 nm SnO_2 shell. In general, the higher response is reported for Au at SnO_2 core–shell nanostructures compared to the pure SnO_2 particles, which may be attributed to the pronounced electronic sensitization, high thermal stability, and low screening effect of Au–Ps.

The 3D nanostructures with their larger surface area and well-organized structure attract much attention due to their

improved gas adsorption and sensing properties (Xia et al., 2018). Li Y.-X. et al. (2016) synthesized shuttle-shaped, cone-shaped, and rod-shaped hierarchical SnO_2 nanostructures *via* hydrothermal approach and demonstrated that cone-shaped nanostructures characterized by the highest response to acetone, ethanol, isopropanol, methanol, etc. remain in good stability and repeatability.

Sensor Arrays

The one of the ways to improve the performance characteristics of semiconductor gas sensor is by the creation of sensor arrays, or so-called electronic nose (e-nose) systems. According to the definition of Gardner and Bartlett (1994), an e-nose is an instrument, which comprises an array of electronic chemical sensors with partial specificity and an appropriate pattern recognition system, capable of recognizing simple or complex odors. The e-nose systems consist of three main elements: matrix of sensing elements, data acquisition system, and software with digital pattern recognition algorithms (Wilson and Baietto, 2009; Ramgir, 2013). **Figure 14** presents the simplified scheme of e-nose system (**Figure 14A**) and illustrative comparison between olfactory system and an e-nose system (**Figure 14B**).

The signal processing of the e-nose system can be described as follows (Ramgir, 2013). The sensitive layers of sensor matrix in contact with gas species cause the change in the electrical characteristics. The data acquisition system captures sensor signals and delivers them to the processing system. The last one is usually presented by microcontroller, digital signal processor, or computer equipped with the appropriate software to process obtained signals. The used data acquisition system must be capable of storing and processing the signals simultaneously from the set of sensors. The software is based on the pattern recognition algorithm, the aim of which is to classify and identify vapors or odors using database with pattern or finger prints from known analytes. To facilitate this process, graphical analysis, multivariate data analysis, or network analysis can be used.

Electronic noses combine gas sensors with different sensitivity and selectivity, and compared to the single MOx gas sensors can consist of sensing elements with lower performance characteristics (Boeker, 2014). Measurement results from each individual sensor are collectively assembled and integrated to produce a digital response pattern, the unique electronic fingerprint of the collective sensor responses to the certain analytes. The sensor responses of different sensing elements usually are presented in the diagram form (**Figure 12**). Such result presentation is very convenient for the selectivity estimating of individual sensors to the same analyte.

To the main advantages of the semiconducting sensor arrays belong very high sensitivity, limited sensing range, rapid response, and recovery times (Wilson and Baietto, 2009). The creation of sensor array systems with a high sensing performance based on the commercially available MOx gas sensors (Penza et al., 2011; Fonollosa et al., 2015; Gebicki and Szulczyński, 2018) and on self-produced sensitive layers (Lee et al., 2002; Krivetsky et al., 2009; Abadi et al., 2011; Peng et al., 2019) have been already highlighted in the literature. For instance, the combination in one device MOx based on sensitive layers with different additives effects strongly on the sensing performance. Thus, Lee et al. (2002) fabricated sensor array consisting of nine metal oxide semiconductor gas sensors based on SnO_2 sensitive layers. The good selectivity of sensors was achieved by doping SnO_2 NPs with Pt, Pd, Au, CuO, La_2O_3, Sc_2O_3, TiO_2, WO_3, and ZnO. The resulting sensor array showed high sensitivity and long-term stability to low gas concentration at 400°C. Peng et al. (2019) showed that the use of various additives contributing to improve sensitivity and recognition ability of the gas sensor array ZnO/SnO_2-based thin films to CO, NO_x, and SO_2. Gwizdz et al. (2014) studied the influence of chromium concentration on the sensing characteristics of TiO_2-based sensor array. It was shown that the change of conductivity from n-type to p-type occurs for the sensitive TiO_2 layer consisting 1% Cr, and the 5% Cr TiO_2 exhibits the highest sensor response to hydrogen.

Carbon Integrated MOx

Another effective way to improve the gas sensing properties of the semiconducting oxides is to integrate the NP or nanostructures on carbon-based functional materials such as the reduced graphene oxide (rGO) and the multi-walled carbon NT (MWCNT) with fast electron transport dynamic, high surface area ratio, and unique electrical and mechanical properties.

For some specific application such as breath analysis, the characteristics of semiconductor sensors (size, phase composition, and structure) need to be tailored during their synthesis and processing. First, sensors should exhibit a high sensitivity to the low concentrations of analyte gases that are present in the breath, ranging from ppt to ppm. Second, selectivity is crucial for the detection of a specific analyte (breath marker) due to the large number of similar compounds present in the human breath. Third, the sensors also need to be able to work at the high relative humidity of the breath (90%) and to be robust to its fluctuations. Last but not the least, the sensors must exhibit rapid response and recovery times at room temperature for fast and on-line measurements.

To meet these requirements, more and more researchers have been focusing on the gas sensors based on two-dimensional (2D) nanostructured materials (graphene and its derivatives, transition metal dichalcogenides) and metal oxide hybrids, which may enhance the sensing performance at room temperature. In fact, the resulting new materials will take advantage of the collective benefits of 2D materials and MOxs. First, for geometrical effects, the construction of a hierarchical structure prevents the agglomeration or restacking of 2D materials or MOxs, which enlarges the active surface area for the reaction with analytes. The porous and controlled nanostructure by the incorporation of MOxs to 2D materials during the synthesis facilitates gas absorption and diffusion corresponding to fine-tuning of the MOx gas response. Second, for the electronic effects, the potential energy barrier and charge carrier depletion zone at the heterojunction can be modulated by gas adsorption and desorption to act as additional reaction sites. The built-in internal electric field formed at the interface promotes additional oxygen adsorption and the conveyance of charge carrier. Third, for the chemical effects, the chemical bonds created between 2D material and MOxs can act as efficient

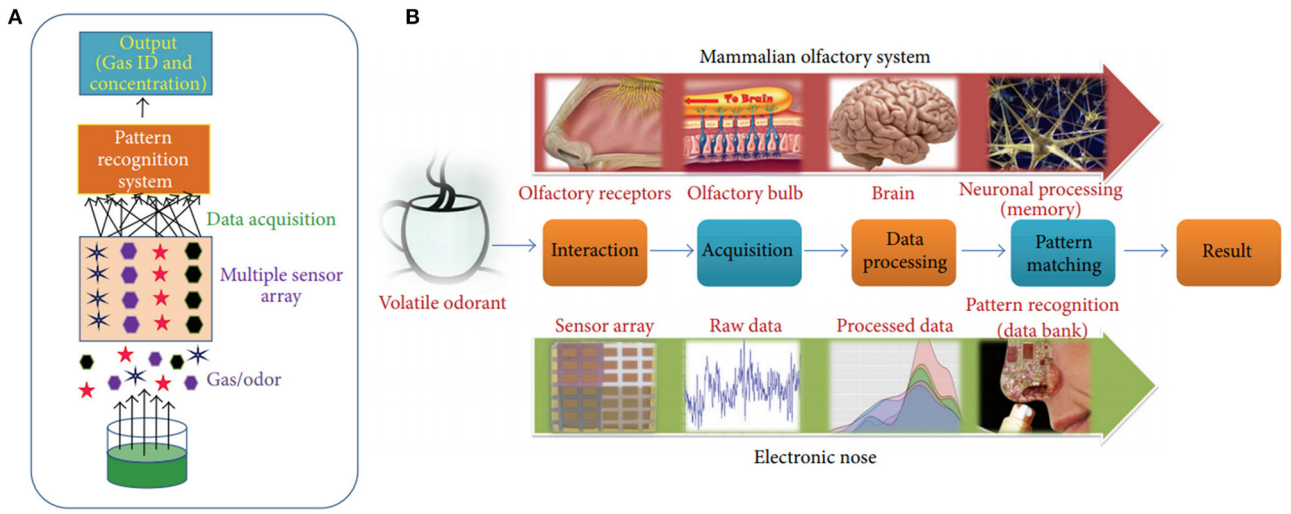

FIGURE 14 | (A) Schematic of a simplified and complete e-nose. **(B)** Schematic comparison of olfactory system and an electronic nose (reproduced from Ramgir, 2013).

charge transport bridges during the gas sensing process. The density of chemisorbed oxygen on the surface of MOxs can be increased by the interfacial chemical bonds. The receptor function of MOxs can improve selective adsorption of analytes. Depending on the MOx used as decorating material and also the type of 2D materials (graphene and its derivatives, transition metal dichalcogenides), the performance of sensor based on this material can be optimized for a specific target gas (Chatterjee et al., 2015; Lee et al., 2018; Sun et al., 2018).

For instance, Tonezzer et al. (2019) used the gas sensor based on carbon-modified NWs grown by chemical vapor deposition to improve gas selectivity. The created device was able to distinguish all tested gases (acetone, ammonia, carbon monoxide, ethanol, hydrogen, and toluene) at low concentration. Moreover, gas sensor based on C–SnO_2 nanostructures works at lower temperature in comparison with pure SnO_2 and has better response and perfect gas classification.

Seekaew et al. (2019) showed a great perspective of Sn–TiO_2 at rGO/CNT nanocomposite for gas sensing applications. In their work, they synthesized carbon modified tin–titanium dioxide, which exhibits ultrahigh NH_3 selectivity, high response, relatively short response, and recovery times. Moreover, device is able to detect ammonia at room temperature and shows good repeatability of results.

CONCLUSIONS AND FUTURE PERSPECTIVE

This review described the most recent studies on SMOxs and their applications as gas sensors. Due to their unique intrinsic properties in terms of chemical, physical, optical, and electronic characteristics, they have already attracted the attention of researchers to use as gas sensing materials with high detection range, reaching to ppb levels. Over the last two decades, it has been proven that the SMOxs synthesized in various morphologies, sizes, and crystal and microstructures becoming more capable for detecting a variety of gases, such as H_2, NO_2, CO, NH_3, O_2, VOCs, NO, SO_2, and H_2S with high sensitivity, selectivity, and stability at a broad temperature range. The induced characteristics offer large specific surface area, superior electron transport rate, extraordinary permeability, and active reaction sites. Thus, it has been possible to detect gases more sensitively and selectively with sensors stable and capable at room temperature, at intermediate temperatures, and even at elevated temperatures well-exceeding 500°C.

The morphologies achieved so far are versatile and can be categorized as 0D (e.g., spheres particles with preferential planes), 1D (e.g., rods and wires), NTs, films, and loaded on 2D supports such as graphene. 0D nanostructured MOxs are prone to the occurrence of superficial chemical reactions at high rates, relying on their large specific surface areas and thus enabling the gas detection with fast respond/recovery time. The 1D nanostructured SMOxs are primarily capable of accelerating the rate of electron transport and consequently results in enhanced gas sensitivity.

It has been demonstrated that the gas sensing properties can be extensively improved by the employment of some other strategies, such as loading with NMs, bulk doping with elements, constructing heterojunctions, and compounding with other functional materials. NPs of SMOxs that are decorated with NMs on their surfaces can change the electron accumulation and enhance catalytic effect resulting in electronic and chemical excitation, respectively. Bulk dopants incorporated to the lattice of the semiconducting oxides change their crystal and electronic structure reducing the band width and increase the surface-active sites that affect the sensitivity and selectivity of the gas sensors.

Other strategies that offers the potential for achievement of better gas sensing materials include construction of heterojunctions and compounds by incorporating with other functional materials. Through the formation of heterojunctions, the electron transfer at the contact surface of the two materials can be effectively rectified yielding improved sensitivity. High resistivity of SMOxs is one of the limitations in respect of better sensor properties. The composite of SMOxs with other functional materials is expected to overcome this and result in high gas response at lower temperatures attributable to possible synergy effects as well as defect structures.

Despite all these achieve advances, some deficiencies exist that requires more research and development in terms of tuning the selectivity, sensitivity, and working temperature for each relevant gas. One of the greatest challenges is related to the selectivity in the presence of several gas species. Current studies report some improvement, however despite tailoring, the SMOx sensing materials, though low, still give response to other specious along with the target gas. The efforts can be devoted into the compositional coordination of nanostructures and components and the development of novel MOx composites and the ease of manufacturing of nanostructured sensors in order to enable their practical applications.

Hence, the future research must be dedicated to evaluating material characteristics for the highest selectivity under different environmental conditions with faster response/recovery time. Additional efforts are needed in tuning long-term stability and adoption of nanotechnological processing to gas sensor manufacturing.

AUTHOR CONTRIBUTIONS

BS has edited TiO_2 based nanotubular and doped gas sensor materials. RLF has edited TiO_2 based nanoparticulate and doped gas sensor materials and sensing mechanisms. SN has edited SnO_2 based nanoparticles and nanostructures and heterostructures and composite gas sensor materials. BS and SN have carried the final reviewing and editing. All authors contributed equally in their specialty areas.

FUNDING

DLR - DAAD Research Fellowships is a program implemented by the German Aerospace Center (DLR) and the German Academic Exchange Service (DAAD) for outstanding scientists and researchers to conduct special research at the institutes of the DLR in Germany. The Library Division of DLR supports the Open Access Publication.

ACKNOWLEDGMENTS

The grants provided by the DLR-DAAD Post-Doctoral Fellowship Program to RLF and SN under no. 284 and no. 441, respectively, are gratefully acknowledged.

REFERENCES

Abadi, M. H. S., Hamidon, M. N., Shaari, A. H., Norhafizah, A., and Rahman, W. (2011). SnO_2/Pt thin film laser ablated gas sensor array. *Sensors* 11, 7724–7735. doi: 10.3390/s110807724

Ahlers, S., Müller, G., and Doll, T. (2005). A rate approach to the gas sensitivity of thin film metal oxide materials. *Sens. Actuators B* 107, 587–599. doi: 10.1016/j.snb.2004.11.020

Akbar, S. A., Dutta, P., and Lee, C. (2006). High-temperature ceramic gas sensors: a review. *Int. J. Appl. Ceramic Technol.* 3, 302–311. doi: 10.1111/j.1744-7402.2006.02084.x

Allam, N. K., and Grimes, C. A. (2008). Effect of cathode material on the morphology and photoelectrochemical properties of vertically oriented TiO_2 nanotube arrays. *Solar Energy Mater. Solar Cells* 92, 1468–1475. doi: 10.1016/j.solmat.2008.06.007

Angkaew, S., and Limsuwan, P. (2012). Preparation of silver-titanium dioxide core-shell (Ag@TiO_2) nanoparticles: effect of Ti-Ag mole ratio. *Procedia Eng.* 32, 649–655. doi: 10.1016/j.proeng.2012.01.1322

Arafat, M. M., Haseeb, A. S. M. A., Akbar, S. A., and Quadir, M. Z. (2017). *In-situ* fabricated gas sensors based on one dimensional core-shell TiO_2-Al_2O_3 nanostructures. *Sens. Actuators B* 238, 972–984. doi: 10.1016/j.snb.2016.07.135

Ayesh, A. (2016). Metal/metal-oxide nanoclusters for gas sensor applications. *J. Nanomater.* 2016:2359019. doi: 10.1155/2016/2359019

Bao, Y., Wei, P., Xia, X., Huang, Z., Homewood, K., and Gao, Y. (2019). Remarkably enhanced H_2 response and detection range in Nb doped rutile/anatase heterophase junction TiO_2 thin film hydrogen sensors. *Sens. Actuators B* 301:127143. doi: 10.1016/j.snb.2019.127143

Barsan, N., and Weimar, U. (2001). Conduction model of metal oxide gas sensors. *J. Electroceramics* 7, 143–167. doi: 10.1023/A:10144058 11371

Batzill, M., and Diebold, U. (2005). The surface and materials science of tin oxide. *Prog. Surf. Sci.* 79, 47–154. doi: 10.1016/j.progsurf.2005.09.002

Bayata, F., Saruhan-Brings, B., and Ürgen, M. (2014). Hydrogen gas sensing properties of nanoporous Al-doped titania. *Sens. Actuators B* 204, 109–118. doi: 10.1016/j.snb.2014.07.079

Beranek, R., Hildebrand, H., and Schmuki, P. (2003). Self-organized porous titanium oxide prepared in H_2SO_4/HF electrolytes. *Electrochem. Solid-State Lett.* 6, B12–B14. doi: 10.1149/1.1545192

Biaggi-Labiosa, A., Solá, F., Lebron-Colon, M., Evans, L., Xu, J., Hunter, G. W., et al. (2012). A novel methane sensor based on porous SnO_2 nanorods: room temperature to high temperature detection. *Nanotechnology* 23:455501. doi: 10.1088/0957-4484/23/45/455501

Bochenkov, V. E., and Sergeev, G. B. (2010). "Sensitivity, selectivity, and stability of gas-sensitive metal-oxide nanostructures" in *Metal Oxide Nanostructures and Their Applications*, eds. A. Umar, and Y.-B. Hang (Valencia, CA: American Scientific Publishers), 31–5.

Boeker, P. (2014). On 'Electronic Nose' methodology. *Sens. Actuators B* 204, 2–17. doi: 10.1016/j.snb.2014.07.087

Brattain, W. H., and Bardeen, J. (1953). Surface properties of germanium. *Bell Syst. Techn. J.* 32, 1–41. doi: 10.1002/j.1538-7305.1953.tb01420.x

Cai, G., Tu, J., Zhou, D., Li, L., Zhang, J., Wang, X., et al. (2014). Constructed TiO_2/NiO core/shell nanorod array for efficient electrochromic epplication. *J. Phys. Chem. C* 118, 6690–6696. doi: 10.1021/jp500699u

Cai, G. F., Zhou, D., Xiong, Q. Q., Zhang, J. H., Wang, X. L., Gu, C. D., et al. (2013). Efficient electrochromic materials based on TiO_2@WO_3 core/shell nanorod arrays. *Solar Energy Mater. Solar Cells* 117, 231–238. doi: 10.1016/j.solmat.2013.05.049

Caricato, A., Buonsanti, R., Catalano, M., Cesaria, M., Cozzoli, D., Luches, A., et al. (2011). Films of brookite TiO_2 nanorods/nanoparticles deposited by matrix-assisted pulsed laser evaporation as NO_2 gas-sensing layers. *Appl. Phys. A* 104, 963–968. doi: 10.1007/s00339-011-6462-5

Chachuli, M. S., Hamidon, M., Mamat, S., Ertugrul, M., and Abdullah, N. (2018). A hydrogen gas sensor based on TiO_2 nanoparticles on alumina substrate. *Sensors* 18:2483. doi: 10.3390/s18082483

Chang, Y.-H., Liu, C.-M., Chen, C., and Cheng, H.-E. (2012). The heterojunction effects of TiO_2 nanotubes fabricated by atomic layer deposition on photocarrier transportation direction. *Nanoscale Res. Lett.* 7:231. doi: 10.1186/1556-276X-7-231

Chatterjee, S. G., Chatterjee, S., Ray, A. K., and Chakraborty, A. K. (2015). Graphene–metal oxide nanohybrids for toxic gas sensor: a review. *Sens. Actuators B* 221, 1170–1181. doi: 10.1016/j.snb.2015.07.070

Chen, N., Deng, D., Li, Y., Liu, X., Xinxin, X., Xuechun, X., et al. (2017). TiO_2 nanoparticles functionalized by Pd nanoparticles for gas-sensing application with enhanced butane response performances. *Sci. Rep.* 7:7692. doi: 10.1038/s41598-017-08074-y

Choi, J.-K., Hwang, I.-S., Kim, S.-J., Park, J.-S., Park, S.-S., Jeong, U., et al. (2010). Design of selective gas sensors using electrospun Pd-doped SnO_2 hollow nanofibers. *Sens. Actuators B* 150, 191–199. doi: 10.1016/j.snb.2010.07.013

Choi, M. G., Lee, Y. G., Song, S. W., and Kim, K. M. (2010). Lithium-ion battery anode properties of TiO_2 nanotubes prepared by the hydrothermal synthesis of mixed (anatase and rutile) particles. *Electrochim. Acta* 55, 5975–5983. doi: 10.1016/j.electacta.2010.05.052

Choi, Y., Hwang, I., Park, J.-G., Choi, K.-J., Park, J.-H., and Lee, J.-H. (2008). Novel fabrication of an SnO_2 nanowire sensor with high sensitivity. *Nanotechnology* 19:095508. doi: 10.1088/0957-4484/19/9/095508

Choopun, S., Hongsith, N., and Wongrat, E. (2012). "Metal-oxide nanowires for gas sensors," in *Nanowires – Recent Advances*, ed. X. Peng (London: IntechOpen), 3–24. doi: 10.5772/54385

Comini, E. (2006). Metal oxide nano-crystals for gas sensing. *Anal. Chim. Acta* 568, 28–40. doi: 10.1016/j.aca.2005.10.069

Comini, E., Faglia, G., Sberveglieri, G., and Pan, Z. (2002). Stable and highly sensitive gas sensors based on semiconducting oxide nanobelts. *Appl. Phys. Lett.* 81, 1869–1871. doi: 10.1063/1.1504867

Dai, Z., Gole, J., Stout, J., and Wang, Z. (2002). Tin oxide nanowires, nanoribbons, and nanotubes. *J. Phys. Chem. B* 106, 1274–1279. doi: 10.1021/jp013214r

Dai, Z., Pan, Z., and Wang, Z. L. (2003). Novel nanostructures of functional oxide synthesized by thermal evaporation. *Adv. Funct. Mater.* 13, 9–24. doi: 10.1002/adfm.200390013

David, T. M., Gnanasekar, K. I., Wilson, P., Sagayaraj, P., and Mathews, T. (2020). Effect of Ni, Pd, and Pt nanoparticle dispersion on thick films of TiO_2 nanotubes for hydrogen ensing: TEM and XPS studies. *ACS Omega* 5, 11352–11360. doi: 10.1021/acsomega.0c00292

Degler, D., Weimar, U., and Barsan, N. (2019). Current understanding of the fundamental mechanisms of doped and loaded semiconducting metal-oxide-based sas sensing materials. *ACS Sens.* 4, 2228–2249. doi: 10.1021/acssensors.9b00975

Dey, A. (2018). Semiconductor metal oxide gas sensors: a review. *Mater. Sci. Eng. B* 229, 206–217. doi: 10.1016/j.mseb.2017.12.036

Ding, X., Zeng, D., and Xie, C. (2010). Controlled growth of SnO_2 nanorods clusters via Zn doping and its influence on gas-sensing properties. *Sens. Actuators B* 149, 336–344. doi: 10.1016/j.snb.2010.06.057

Docquier, N., and Candel, S. (2002). Combustion control and sensors: a review. *Progress Energy Combustion Sci.* 28, 107–150. doi: 10.1016/S0360-1285(01)00009-0

Dong, K.-Y., Choi, J.-K., Hwang, I.-S., Lee, J.-W., Kang, B. H., Ham, D.-J., et al. (2011). Enhanced H_2S sensing characteristics of Pt doped SnO_2 nanofibers sensors with micro heater. *Sens. Actuators B* 157, 154–161. doi: 10.1016/j.snb.2011.03.043

Dubourg, G., Segkos, A., Katona, J., Radović, M., Savić, S., Niarchos, G., et al. (2017). Fabrication and characterization of flexible and miniaturized humidity sensors using screen-printed TiO_2 nanoparticles as sensitive layer. *Sensors* 17:1854. doi: 10.3390/s17081854

Dufour, N., Veyrac, Y., Menini, P., Blanc, F., and Talhi, C. (2012). Increasing the sensitivity and selectivity of metal oxide gas sensors by controlling the sensitive layer polarization. *IEEE Sens.* 2012, 1–4. doi: 10.1109/ICSENS.2012.6411463

El-Maghraby, E. M., Qurashi, A., and Yamazaki, T. (2013). Synthesis of SnO_2 nanowires their structural and H_2 gas sensing properties. *Ceramics Int.* 39, 8475–8480. doi: 10.1016/j.ceramint.2013.01.112

Epifani, M., Andreu, T., Zamani, R., Arbiol, J., Comini, E., Siciliano, P., et al. (2012). Pt doping triggers growth of TiO_2 nanorods: nanocomposite synthesis and gas-sensing properties. *CrystEngComm* 14, 3882–3887. doi: 10.1039/c2ce06690d

Eranna, G. (2012). *Metal Oxide Nanostructures as Gas Sensing Devices*. Boca Raton, FL: CRC Press, 336.

Fields, L. L., Zheng, J. P., Cheng, Y., and Xiong, P. (2006). Room-temperature low-power hydrogen sensor based on a single tin dioxide nanobelt. *Appl. Phys. Lett.* 88:263102. doi: 10.1063/1.2217710

Fonollosa, J., Rodríguez-Luján, I., and Huerta, R. (2015). Chemical gas sensor array dataset. *Data Brief* 3, 85–89. doi: 10.1016/j.dib.2015.01.003

Foong, T. R. B., Shen, Y. D., Hu, X., and Sellinger, A. (2010). Template-directed liquid ALD growth of TiO_2 nanotube arrays: properties and potential in photovoltaic devices. *Adv. Funct. Mater.* 20, 1390–1396. doi: 10.1002/adfm.200902063

Galstyan, V., Comini, E., Faglia, G., and Sberveglieri, G. (2013). Review: TiO_2 nanotubes: recent advances in synthesis and gas sensing properties. *Sensors* 13, 14813–14838. doi: 10.3390/s131114813

Galstyan, V., Comini, E., Faglia, G., Vomiero, A., Borgese, L., Bontempi, E., et al. (2012a). Fabrication and investigation of gas sensing properties of Nb-doped TiO_2 nanotubular arrays. *Nanotechnology* 23:235706. doi: 10.1088/0957-4484/23/23/235706

Galstyan, V., Comini, E., Vomiero, A., Ponzoni, A., Concina, I., Brisotto, M., et al. (2012b). Fabrication of pure and Nb-TiO_2 nanotubes and their functional properties. *J. Alloys Compd.* 536, S488–S490. doi: 10.1016/j.jallcom.2011.12.076

Galstyan, V., Vomiero, A., Comiani, E., Faglia, G., and Sberveglieri, G. (2011). TiO_2 nanotubular and nanoporous arrays by electrochemical anodization on different substrates. *RSC Adv.* 1, 1038–1044. doi: 10.1039/c1ra00077b

Gardner, J. W., and Bartlett, P. N. (1994). A brief history of electronic noses. *Sens. Actuators B* 18, 210–211. doi: 10.1016/0925-4005(94)87085-3

Gebicki, J., and Szulczyński, B. (2018). Discrimination of selected fungi species based on their odour profile using prototypes of electronic nose instruments. *Measurement* 116, 307–313. doi: 10.1016/j.measurement.2017.11.029

Goebl, J., Joo, J. B., Dahl, M., and Yin, Y. (2014). Synthesis of tailored Au@TiO_2 core–shell nanoparticles for photocatalytic reforming of ethanol. *Catalysis Today* 225, 90–95. doi: 10.1016/j.cattod.2013.09.011

Gong, D., Grimes, C. A., Varghese, O. K., Hu, W. C., Singh, R. S., Chen, Z., et al. (2001). Titanium oxide nanotube arrays prepared by anodic oxidation. *J. Mater. Res.* 16, 3331–3334. doi: 10.1557/JMR.2001.0457

Gönüllü, Y., Haidry, A. A., and Saruhan, B. (2015). Nanotubular Cr-doped TiO_2 for use as high-temperature NO_2 gas sensor. *Sens. Actuators B* 217, 78–87. doi: 10.1016/j.snb.2014.11.065

Gönüllü, Y., Kelm, K., Mathur, S., and Saruhan, B. (2014). Equivalent circuit models for determination of the relation between the sensing behavior and properties of undoped/Cr doped TiO_2 NTs. *Chemosensors* 2, 69–84. doi: 10.3390/chemosensors2010069

Gönüllü, Y., Rodriguez, G. C. M., Saruhan, B., and Ürgen, M. (2012). Improvement of gas sensing performance of TiO_2 towards NO_2 by nano-tubular structuring. *Sens. Actuators B* 169, 151–160. doi: 10.1016/j.snb.2012.04.050

Govardhan, K., and Grace, A. (2016). Metal/metal oxide doped semiconductor based metal oxide gas sensors—a review. *Sens. Lett.* 14, 741–750. doi: 10.1166/sl.2016.3710

Gwizdz, P., Radecka, M., and Zakrzewska, K. (2014). Array of chromium doped nanostructured TiO_2 metal oxide gas sensors. *Procedia Eng.* 87, 1059–1062. doi: 10.1016/j.proeng.2014.11.345

Haidry, A., Kind, N., and Saruhan, B. (2015). Investigating the influence of Al-doping and background humidity on NO_2 sensing characteristics of magnetron-sputtered SnO_2 sensors. *J. Sens Sens Syst.* 4, 271–280. doi: 10.5194/jsss-4-271-2015

Haldar, K. K., and Patra, A. (2008). Efficient resonance energy transfer from dye to Au@SnO_2 core–shell nanoparticles. *Chem. Phys. Let.t* 462, 88–91. doi: 10.1016/j.cplett.2008.07.068

Hamanaka, M., Imakawa, K., Yoshida, M., Zhao, Z., Yin, S., Wu, X., et al. (2016). Synthesis and gas sensing properties of SnO_2 nanoparticles with different morphologies. *J. Porous Mater.* 23, 1189–1196. doi: 10.1007/s10934-016-0177-0

Harris, L. A. (1980). A titanium dioxide hydrogen sensor. *J. Electrochem. Soc.* 127, 2657–2662. doi: 10.1149/1.2129567

Hien, V., Vuong, D. D., Chien, N., and Trung, K. (2011). Synthesis of tin dioxide nanoparticles and nanorods by hydrothermal method and

gas sensing characteristics*. *e-J. Surf. Sci. Nanotechnol.* 27, 503–507. doi: 10.1380/ejssnt.2011.503

Hieu, N. V., Kim, H.-R., Ju, B.-K., and Lee, J.-H. (2008). Enhanced performance of SnO_2 nanowires ethanol sensor by functionalizing with La_2O_3. *Sens. Actuators B* 133, 228–234. doi: 10.1016/j.snb.2008.02.018

Huang, J., and Wan, Q. (2009). Gas sensors based on semiconducting metal oxide one-dimensional nanostructures. *Sensors* 9, 9903–9924. doi: 10.3390/s91209903

Huang, Y. J., Pandraud, G., and Sarro, P. M. (2012). The atomic layer deposition array defined by etch-back technique: a new method to fabricate TiO_2 nanopillars, nanotubes and nanochannel arrays. *Nanotechnology* 23:485306. doi: 10.1088/0957-4484/23/48/485306

Ji, H., Zeng, W., and Li, Y. (2019). Gas sensing mechanisms of metal oxide semiconductors: a focus review. *Nanoscale* 11, 22664–22684. doi: 10.1039/C9NR07699A

Jia, C., Dong, T., Li, M., Wang, P., and Yang, P. (2018). Preparation of anatase/rutile TiO_2/SnO_2 hollow heterostructures for gas sensor. *J. Alloys Compd.* 769, 521–531. doi: 10.1016/j.jallcom.2018.08.035

Kanda, T., Komata, K., Torigoe, K., Endo, T., Sakai, K., Abe, M., et al. (2014). Preparation of gold/titania core-shell nanocomposites with a tunable shell thickness. *J. Oleo Sci.* 63, 507–513. doi: 10.5650/jos.ess13203

Kaur, N., Singh, M., Moumen, A., Duina, G., and Comini, E. (2020). Review 1D titanium dioxide: achievements in chemical sensing. *Materials* 13:2974. doi: 10.3390/ma13132974

Khatami, M., Alijani, H. Q., Nejad, M. S., and Varma, R. S. (2018). Core@shell nanoparticles: greener synthesis using natural plant products. *Appl. Sci.* 8:411. doi: 10.3390/app8030411

Khatoon, Z., Fouad, H., Alothman, O. Y., Hashem, M., Ansari, Z. A., and Ansari, S. A. (2020). Doped SnO_2 nanomaterials for e-nose based electrochemical sensing of biomarkers of lung cancer. *ACS Omega* 5, 27645–27654. doi: 10.1021/acsomega.0c04231

Khoang, N. D., Trung, D. D., Duy, N. V., Hoa, N. D., and Hieu, N. V. (2012). Design of SnO_2/ZnO hierarchical nanostructures for enhanced ethanol gas-sensing performance. *Sens. Actuators B* 174, 594–601. doi: 10.1016/j.snb.2012.07.118

Khuc, Q. T., Vu, X. H., Dang, D. V., and Nguyen, D. C. (2010). The Influence of hydrothermal temperature on SnO_2 nanorod formation. *Adv. Natural Sci.* 1:25010. doi: 10.1088/2043-6254/1/2/025010

Kilinc, N., Sennik, E., and Ozturk, Z. Z. (2011). Fabrication of TiO_2 nanotubes by anodization of Ti thin films for VOC sensing. *Thin Solid Films* 520, 953–958. doi: 10.1016/j.tsf.2011.04.183

Kim, H.-J., and Lee, J.-H. (2014). Highly sensitive and selective gas sensors using p-type oxide semiconductors: overview. *Sens. Actuators B* 192, 607–627. doi: 10.1016/j.snb.2013.11.005

Kim, I., and Choi, W. Y. (2017). Hybrid gas sensor having TiO_2 nanotube arrays and SnO_2 nanoparticles. *Int. J. Nanotechnol.* 14, 155–165. doi: 10.1504/IJNT.2017.082459

Kim, W.-S., Lee, B.-S., Kim, D.-H., Kim, H.-C., Yu, W.-R., and Hong, S.-H. (2010). SnO_2 nanotubes fabricated using electrospinning and atomic layer deposition and their gas sensing performance. *Nanotechnology* 21:245605. doi: 10.1088/0957-4484/21/24/245605

Kolmakov, A., Klenov, D. O., Lilach, Y., Stemmer, S., and Moskovits, M. (2005). Enhanced gas sensing by individual SnO_2 nanowires and nanobelts functionalized with Pd catalyst particles. *Nano Lett.* 5, 667–673. doi: 10.1021/nl050082v

Kong, X., and Li, Y. (2005). High sensitivity of CuO modified SnO_2 nanoribbons to H_2S at room temperature. *Sens. Actuators B* 105, 449–453. doi: 10.1016/j.snb.2004.07.001

Koo, W.-T., Jang, J.-S., Choi, S.-J., Cho, H.-J., and Kim, I.-D. (2017). Metal-organic framework templated catalysts: dual sensitization of PdO-ZnO composite on hollow SnO_2 nanotubes for selective acetone sensors. *ACS Appl. Mater. Interfaces* 9, 18069–18077. doi: 10.1021/acsami.7b04657

Korotcenkov, G., Brinzari, V., and Cho, B. K. (2016). Conductometric gas sensors based on metal oxides modified with gold nanoparticles: a review. *Microchim. Acta* 183, 1033–1054. doi: 10.1007/s00604-015-1741-z

Krivetskiy, V. V., Rumyantseva, M. N., and Gaskov, A. M. (2013). Chemical modification of nanocrystalline tin dioxide for selective gas sensors. *Russian Chem. Rev.* 82, 917–941. doi: 10.1070/RC2013v082n10ABEH004366

Krivetsky, V., Ponzoni, A., Comini, E., Rumyantseva, M., and Gaskov, A. (2009). Selective modified SnO_2-based materials for gas sensors arrays. *Procedia Chem.* 1, 204–207. doi: 10.1016/j.proche.2009.07.051

Kumar, M., Kumar, D., and Gupta, A. (2015). Fe-doped TiO_2 thin films for CO gas sensing. *J. Electron. Mater.* 44, 152–157. doi: 10.1007/s11664-014-3477-7

Kumar, V., Sen, S., Muthe, K. P., Gaur, N. K., Gupta, S. K., and Yakhmi, J. V. (2009). Copper doped SnO_2 nanowires as highly sensitive H_2S gas sensor. *Sens. Actuators B* 138, 587–590. doi: 10.1016/j.snb.2009.02.053

Kwon, Y., Kim, H., Lee, S., Chin, I. J., Seong, T. Y., Lee, W. I., et al. (2012). Enhanced ethanol sensing properties of TiO_2 nanotube sensors. *Sens. Actuators B* 173, 441–446. doi: 10.1016/j.snb.2012.07.062

Lai, C. W., and Sreekantan, S. (2013). Incorporation of WO_3 species into TiO_2 nanotubes via wet impregnation and their water-splitting performance. *Electrochim. Acta* 87, 294–302. doi: 10.1016/j.electacta.2012.09.022

Lai, M., Lim, J.-H., Hussaini, J. S. M., Youngwo, R., Mulchandani, A., Deshusses, M., et al. (2009). Size-controlled electrochemical synthesis and properties of SnO_2 nanotubes. *Nanotechnology* 20:185602. doi: 10.1088/0957-4484/20/18/185602

Lai, Y., Zhuang, H., Sun, L., Chen, Z., and Lin, C. (2009). Self-organized TiO_2 nanotubes in mixed organic-inorganic electrolytes and their photoelectrochemical performance. *Electrochim. Acta* 54, 6536–6542. doi: 10.1016/j.electacta.2009.06.029

Landau, O., Rothschild, A., and Zussman, E. (2009). Processing-microstructure-properties correlation of ultrasensitive gas sensors produced by electrospinning. *Chem. Mater.* 21, 9–11. doi: 10.1021/cm802498c

Law, M., Kind, H., Messer, B., Kim, F., and Yang, P. (2002). Photochemical sensing of NO_2 with SnO_2 nanoribbon nanosensors at room temperature. *Angew. Chem.* 41, 2405–2408. doi: 10.1002/1521-3757(20020703)114:13<2511::AID-ANGE2511>3.0.CO;2-N

Lee, D.-S., Lee, D.-D., Ban, S.-W., Lee, M., and Kim, Y. (2002). SnO_2 gas sensing array for combustible and explosive gas leakage recognition. *Sens. J. IEEE* 2, 140–149. doi: 10.1109/JSEN.2002.800685

Lee, E., Yoon, Y. S., and Kim, D.-J. (2018). Two-dimensional transition metal dichalcogenides and metal oxide hybrids for gas sensing. *ACS Sens.* 3, 2045–2060. doi: 10.1021/acssensors.8b01077

Lee, J., Kim, D. H., Hong, S. H., and Jho, J. Y. (2011). A hydrogen gas sensor employing vertically aligned TiO_2 nanotube arrays prepared by template-assisted method. *Sens. Actuators B* 160, 1494–1498. doi: 10.1016/j.snb.2011.08.001

Li, L., Zhang, C., and Chen, W. (2015). Fabrication of SnO_2-SnO nanocomposites with p-n heterojunctions for low-temperature sensing of NO_2 gas. *Nanoscale* 7, 12133–12142. doi: 10.1039/C5NR02334C

Li, S.-H., Meng, F.-F., Chu, Z., Luo, T., Peng, F.-M., and Jin, Z. (2017). Mesoporous SnO_2 nanowires: synthesis and ethanol sensing properties. *Adv. Condensed Matter. Phys.* 2017:9720973. doi: 10.1155/2017/9720973

Li, T., Zeng, W., and Zhao, W. (2016). Gas sensing performance of multiple SnO_2 1D nanostructures based on their interconnect manner. *Mater. Lett.* 167, 230–233. doi: 10.1016/j.matlet.2016.01.013

Li, Y.-X., Guo, Z., Su, Y., Jin, X.-B., Tang, X.-H., Huang, J.-R., et al. (2016). Hierarchical morphology-dependent gas-sensing performances of three-dimensional SnO_2 nanostructures. *ACS Sens.* 2, 102–110. doi: 10.1021/acssensors.6b00597

Li, Z., Ding, D., Liu, Q., and Ning, C. (2013). Hydrogen sensing with Ni-doped TiO_2 nanotubes. *Sensors* 13, 8393–8402. doi: 10.3390/s130708393

Li, Z., Ding, D., Liu, Q., Ning, C., and Wang, X. (2014). Ni-doped TiO_2 nanotubes for wide-range hydrogen sensing. *Nanoscale Res. Lett.* 9:118. doi: 10.1186/1556-276X-9-118

Liang, F. X., Luo, L. B., Tsang, C. K., Zheng, L. X., Cheng, H., and Li, Y. Y. (2012). TiO_2 nanotube-based field effect transistors and their application as humidity sensors. *Mater. Res. Bull.* 47, 54–58. doi: 10.1016/j.materresbull.2011.10.006

Liang, Y.-C., Liao, W.-K., and Deng, X.-S. (2014). Synthesis and substantially enhanced gas sensing sensitivity of homogeneously nanoscale Pd- and Au-particle decorated ZnO nanostructures. *J. Alloys Compd.* 599, 87–92. doi: 10.1016/j.jallcom.2014.01.167

Lin, S., Li, D., Wu, J., Li, X., and Akbar, S. A. (2011). A selective room temperature formaldehyde gas sensor using TiO_2 nanotube arrays. *Sens. Actuators B* 156, 505–509. doi: 10.1016/j.snb.2011.02.046

Liu, D., Lin, L., Chen, Q., Zhou, H., and Wu, J. (2017). Low power consumption gas sensor created from silicon nanowires/TiO_2 core–shell heterojunctions. *ACS Sens.* 2, 1491–1497. doi: 10.1021/acssensors.7b00459

Liu, H. G., Ding, D. Y., Ning, C. Q., and Li, Z. H. (2012). Wide-range hydrogen sensing with Nb-doped TiO_2 nanotubes. *Nanotechnology* 23:015502. doi: 10.1088/0957-4484/23/1/015502

Liu, X., Pan, K., Wang, L., Dong, C., Xiao, X., and Wang, Y. (2015). Butane detection: W-doped TiO_2 nanoparticles for a butane gas sensor with high sensitivity and fast response/recovery. *RSC Adv.* 5, 96539–96546. doi: 10.1039/C5RA20886F

Liu, Y., Huang, J., Yang, J., and Wang, S. (2017). Pt nanoparticles functionalized 3D SnO_2 nanoflowers for gas sensor application. *Solid State Electron.* 130, 20–27. doi: 10.1016/j.sse.2017.01.005

Lontio Fomekong, R., Kelm, K., and Saruhan, B. (2020). High-temperature hydrogen sensing performance of Ni-doped TiO_2 prepared by co-precipitation method. *Sensors* 20:5992. doi: 10.3390/s20215992

Lontio Fomekong, and Saruhan, B. (2019). Synthesis of Co^{3+} doped TiO_2 by co-precipitation route and its gas sensing properties. *Front. Mater.* 6:252. doi: 10.3389/fmats.2019.00252

Lu, H. F., Li, F., Liu, G., Chen, Z. G., Wang, D. W., Fang, H. T., et al. (2008). Amorphous TiO_2 nanotube arrays for low-temperature oxygen sensors. *Nanotechnology* 19:405504. doi: 10.1088/0957-4484/19/40/405504

Lyson-Sypien, B., Czapla, A., Lubecka, M., Gwizdz, P., Schneider, K., Zakrzewska, K., et al. (2012). Nanopowders of chromium doped TiO_2 for gas sensors. *Sens. Actuators B* 175, 163–172. doi: 10.1016/j.snb.2012.02.051

Lyson-Sypien, B., Kusior, A., Rekas, M., Zukrowski, J., and Gajewska, M., Michalow-Mauke, K., et al. (2017). Nanocrystalline TiO_2/SnO_2 heterostructures for gas sensing. *Beilstein J. Nanotechnol.* 8, 108–122. doi: 10.3762/bjnano.8.12

Majhi, S. M., Naik, G. K., Lee, H.-J., Song, H.-G., Lee, C.-R., Lee, I.-H., et al. (2018). Au@NiO core-shell nanoparticles as a p-type gas sensor: novel synthesis, characterization, and their gas sensing properties with sensing mechanism. *Sens. Actuators B* 268, 223–231. doi: 10.1016/j.snb.2018.04.119

Maziarz, W. (2019). TiO_2/SnO_2 and TiO_2/CuO thin film nano-heterostructures as gas sensors. *Appl. Surf. Sci.* 480, 362–370. doi: 10.1016/j.apsusc.2019.02.139

Miller, T. A., Bakrania, S. D., Perez, V., and Wooldridge, M. S. (2006). "Nanosturctured tin dioxide materials for gas sensor applications," in *Functional Nanomaterials*, eds K. E. Geckeler and E. Rosenberg (Valencia, CA: American Scientific Publishers), 1–24. doi: 10.5840/questions200661

Miyaji, A., Ogura, S., Konishi, S., and Tamaki, J. (2004). Effect of micro-gap electrode in nitrogen dioxide sensor using tungsten oxide thin film. *Proc. Electrochem. Soc.* 9, 201–208. doi: 10.1016/j.snb.2004.09.047

Morrison, R. S. (1987). Mechanism of semiconductor gas sensor operation. *Sens. Actuat.* 11, 283–287. doi: 10.1016/0250-6874(87)80007-0

Müller, R., Hernandez-Ramirez, F., Shen, H., Du, H., Mader, W., and Mathur, S. (2012). Influence of precursor chemistry on morphology and composition of CVD-Grown SnO_2 nanowires. *Chem. Mater.* 24, 4028–4035. doi: 10.1021/cm300913h

Nahirniak, S., and Dontsova, T. (2017). "Gas sensor device creation," *2017 IEEE 7th International Conference on Nanomaterials: Applications and Properties (NAP-2017)* (Ukraine), 01NNPT13-1–4. doi: 10.1109/NAP.2017.8190193

Nakate, U., Patil, P., Na, S., Yu, Y., Suh, E.-K., and Hahn, Y. (2020). Fabrication and enhanced carbon monoxide gas sensing performance of p-CuO/n-TiO_2 heterojunction device. *Colloids Surf A Physicochem. Eng. Aspects* 612:125962. doi: 10.1016/j.colsurfa.2020.125962

Oldfield, G., Ung, T., and Mulvaney, P. (2000). Au@SnO_2 core-shell nanocapacitors. *Adv. Mater.* 12, 1519–1522. doi: 10.1002/1521-4095(200010)12:20<1519::AIDADMA1519>3.0.CO;2-W

Osnat, L., and Avner, R. (2015). Fibrous TiO_2 gas sensors produced by electrospinning. *J. Electroceramics* 35, 148–159. doi: 10.1007/s10832-015-0007-9

Pan, J., Shen, H., and Mathur, S. (2012). One-dimensional SnO_2 nanostructures: synthesis and applications. *J. Nanotechnol.* 2012:917320. doi: 10.1155/2012/917320

Park, S., An, S., Mun, Y., and Lee, C. (2013). UV-enhanced NO_2 gas sensing properties of SnO_2-Core/ZnO-shell nanowires at room temperature. *ACS Appl. Mater. Interfaces* 5, 4285–4292. doi: 10.1021/am400500a

Partridge, J., Field, M., Sadek, A., Kalantar-zadeh, K., Plessis, J., Taylor, M., et al. (2009). Fabrication, structural characterization and testing of a nanostructured tin oxide gas sensor. *Sens. J. IEEE* 9, 563–568. doi: 10.1109/JSEN.2009.2016613

Patil, S., Patil, A., Dighavkar, C., Thakare, K., Borse, R., Nandre, S., et al. (2015). Semiconductor metal oxide compounds based gas sensors: a literature review. *Front. Mater. Sci.* 9, 14–37. doi: 10.1007/s11706-015-0279-7

Peng, M., Lv, D., Xiong, D., Shen, W., Song, W., and Tan, R. (2019). Facile preparation of a ZnO/SnO_2-based gas sensor array by inkjet printing for gas analysis with BPNN. *J. Electron. Mater.* 48, 2373–2381. doi: 10.1007/s11664-019-06938-9

Penza, M., Domenico, S., Gennaro, C., Rossi, R., Marco, A., Pfister, V., et al. (2011). A gas sensor array for environmental air monitoring: a study case of application of artificial neural networks. *AIP Conf. Proc.* 1362, 205–206. doi: 10.1063/1.3626360

Perillo, P. M., and Rodriguez, D. F. (2012). The gas sensing properties at room temperature of TiO_2 nanotubes by anodization. *Sens. Actuators B* 171, 639–643. doi: 10.1016/j.snb.2012.05.047

Phanichphant, S., Liewhiran, C., Wetchakun, K., Wisitsoraat, A., and Tuantranont, A. (2011). Flame-made Nb-doped TiO_2 ethanol and acetone sensors. *Sensors* 11, 472–484. doi: 10.3390/s110100472

Poloju, M., Jayababu, N., Manikandan, E., and Ramana Reddy, M. V. (2017). Enhancement of the isopropanol gas sensing performance of SnO_2/ZnO core/shell nanocomposites. *J. Mat. Chem.* 10, 2662–2668. doi: 10.1039/C6TC05095F

Postica, V., Vahl, A., Strobel, J., Santos-Carballal, D., Lupan, O., Abdelaziz, C.-E., et al. (2018). Tuning doping and surface functionalization of columnar oxide films for volatile organic compounds sensing: xperiments and theory. *J. Mater. Chem A* 6, 23669–23682. doi: 10.1039/C8TA08985J

Qi, Q., Zhang, T., Zheng, X., Fan, H., Liu, L., Wang, R., et al. (2008). Electrical response of Sm_2O_3-doped SnO_2 to C_2H_2 and effect of humidity interference. *Sens. Actuators B* 134, 36–42. doi: 10.1016/j.snb.2008.04.011

Qian, L., Wang, K., Li, Y., Fang, H., Lu, Q., and Ma, X. (2006). CO sensor based on Au-decorated SnO_2 nanobelt. *Mater. Chem. Phys.* 100, 82–84. doi: 10.1016/j.matchemphys.2005.12.009

Radecka, M., Kusior, A., Łacz, A., Trenczek-Zajac, A., Lyson-Sypien, B., and Zakrzewska, K. (2011). Nanocrystalline TiO_2/SnO_2 composites for gas sensors. *J. Therm. Anal. Calorim.* 108, 1–6. doi: 10.1007/s10973-011-1966-y

Rai, P., Sanjit, M., Yu, Y., and Lee, J.-H. (2015). Noble metal@metal oxide semiconductor core@shell nano-architectures as a new platform for gas sensor applications. *RSC Adv.* 5, 76229–76248. doi: 10.1039/C5RA14322E

Ramgir, N. S. (2013). Electronic nose based on nanomaterials: issues, challenges, and prospects. *IRSN Nanomater.* 2013:941581. doi: 10.1155/2013/941581

Rane, S., Arbuj, S., Rane, S., and Gosavi, S. (2015). Hydrogen sensing characteristics of Pt–SnO_2 nano-structured composite thin films. *J. Mater. Sci.* 26, 3707–3716. doi: 10.1007/s10854-015-2889-3

Raza, M. H., Kaur, N., Comini, E., and Pinna, N. (2020). Toward optimized radial modulation of the space-charge region in one-dimensional SnO_2-NiO core–shell nanowires for hydrogen sensing. *ACS Appl. Mater. Interfaces* 12, 4594–4606. doi: 10.1021/acsami.9b19442

Romppainen, P. (1997). *Electrical Studies on the Response Characteristics of Tin Dioxide-Bases Semiconductor Gas Sensors*. Oulu, University of Oulu.

Ruiz, A. M., Sakai, G., Cornet, A., Shimanoe, K., Morante, J. R., and Yamazoe, N. (2003). Cr-doped TiO_2 gas sensor for exhaust NO_2 monitoring. *Sens. Actuators B* 93, 509–518. doi: 10.1016/S0925-4005(03)00183-7

Sadeghzade-Attar, A. (2019). Preparation and enhanced photocatalytic activity of Co/F codoped tin oxide nanotubes/nanowires: a wall thickness-dependence study. *Appl. Phys. A* 125:768. doi: 10.1007/s00339-019-2994-x

Sakai, H., Kanda, T., Shibata, H., Ohkubo, T., and Abe, M. (2006). Preparation of highly dispersed core/shell-type titania nanocapsules containing a single Ag nanoparticle. *J. Am. Chem. Soc.* 128 , 4944–4945. doi: 10.1021/ja058083c

Salehi, A. (2008). Selectivity enhancement of indium-doped SnO_2 gas sensors. *Thin Solid Films* 416, 260–263. doi: 10.1016/S0040-6090(02)00626-0

Saruhan, B., Haidry, A. A., Yüce, A., Ciftyürek, E., and Mondragón Rodríguez, G. C. (2016). A p-type double layer "$BaTi_{(1-x)}Rh_xO_3$/Al-doped TiO_2" sensing electrode for NO_2-detection above 600 °C. *Chemosensors* 4, 8–24. doi: 10.3390/chemosensors4020008

Saruhan, B., Yüce, A., Gönüll,ü, Y., and Kelm, K. (2013). Effect of aluminium doping on NO_2 gas sensing of TiO_2 at elevated temperatures. *Sens. Actuators B* 187, 586–597. doi: 10.1016/j.snb.2013.04.111

Sayago, I., Fernández, M. J., Fontecha, J. L., Horrillo, M. C., and Santos, J. (2015). "Synthesis and characterization of SnO_2 nanowires grown by CVD for application as gas sensors," *Proceedings of the 2015 10th Spanish Conference on Electron Devices, CDE*. doi: 10.1109/CDE.2015.7087486

Seekaew, Y., Pon-On, W., and Wongchoosuk, C. (2019). Ultrahigh selective room-temperature ammonia gas sensor based on tin–titanium dioxide/reduced graphene/carbon nanotube nanocomposites by the solvothermal method. *ACS Omega* 4, 16916–16924. doi: 10.1021/acsomega.9b02185

Sennik, E., Colak, Z., Kilinc, N., and Ozturk, Z. Z. (2010). Synthesis of highly-ordered TiO_2 nanotubes for a hydrogen sensor. *Int. J. Hydrogen Energy* 35, 4420–4427. doi: 10.1016/j.ijhydene.2010.01.100

Seo, M.-H., Yuasa, M., Kida, T., Huh, J.-S., Shimanoe, K., and Yamazoe, N. (2009). Gas sensing characteristics and porosity control of nanostructured films composed of TiO_2 nanotubes. *Sens. Actuators B* 137, 513–520. doi: 10.1016/j.snb.2009.01.057

Shaalan, N., Yamazaki, T., and Kikuta, T. (2011). Effect of micro-electrode geometry on NO_2 gas-sensing characteristics of one-dimensional tin dioxide nanostructure microsensors. *Sens. Actuators B* 156, 784–790. doi: 10.1016/j.snb.2011.02.039

Shamsudin, S., Yahaya, M., and Salleh, M. M. (2002). The effect of dopants on the sensing selectivity of SnO_2 thin films-based gas sensors. *ICSE Proce.* 2002, 455–457. doi: 10.1109/SMELEC.2002.1217864

Shanmugasundaram, A., Basak, P., Satyanarayana, L., and Sunkara, M. (2013). Hierarchical SnO/SnO_2 nanocomposites: formation of in situ p–n junctions and enhanced H_2 sensing. *Sens. Actuators B* 185, 265–273. doi: 10.1016/j.snb.2013.04.097

Shao, F., Hoffmann, M. W. G., Prades, J. D., Zamani, R., Arbiol, J., Morante, J. R., et al. (2013). Heterostructured p-CuO (nanoparticle)/n-SnO_2 (nanowire) devices for selective H_2S detection. *Sens. Actuators B* 181, 130–135. doi: 10.1016/j.snb.2013.01.067

Shaposhnik, A. V., Shaposhnik, D. A., Turishchev, S. Y., Chuvenkova, O. A., Ryabtsev, S. V., Vasiliev, A. A., et al. (2019). Gas sensing properties of individual SnO_2 nanowires and SnO_2 sol-gelnanocomposites. *Beilstein J. Nanotechnol.* 10, 1380–1390. doi: 10.3762/bjnano.10.136

Sharma, B., Sharma, A., Joshi, M., and Myung,. J.-,h. (2020). Sputtered SnO_2/ZnO heterostructures for improved NO_2 gas sensing properties. *Chemosensors* 8:67. doi: 10.3390/chemosensors8030067

Sharma, R. K., Bhatnagar, M. C., and Sharma, G. L. (1996). Effect of Nb metal ion in TiO_2 oxygen gas sensor. *Appl. Surf. Sci.* 92, 647–650. doi: 10.1016/0169-4332(95)00311-8

Sharma, R. K., Bhatnagar, M. C., and Sharma, G. L. (1998). Mechanism in Nb doped titania oxygen gas sensor. *Sens. Actuators B* 46, 194–201. doi: 10.1016/S0925-4005(98)00111-7

Shehzad, K., Shah, N., Amin, M., Abbas, M., and Syed, W. (2018). Synthesis of SnO_2 nanowires for CO, CH_4 and CH_3OH gases sensing. *Int. J. Distribut. Sens. Networks* 14:155014771879075. doi: 10.1177/1550147718790750

Shen, R., Li, X., Xia, X., Liang, H., Wu, G., Liu, Y., et al. (2012). Comparative investigation of three types of ethanol sensor based on NiO-SnO_2 composite nanofibers. *Chinese Sci. Bull.* 57, 2087–2093. doi: 10.1007/s11434-012-5105-3

Shen, Y., Wang, W., Fan, A., Wei, D., Liu, W., Han, C., et al. (2015). Highly sensitive hydrogen sensors based on SnO_2 nanomaterials with different morphologies. *Int. J. Hydrogen Energy* 40, 15773–15779. doi: 10.1016/j.ijhydene.2015.09.077

Shen, Y., Yamazaki, T., Liu, Z., Meng, D., Kikuta, T., Nakatani, N., et al. (2009). Microstructure and H_2 gas sensing properties of undoped and Pd-doped SnO_2 nanowires. *Sens. Actuators B* 135, 524–529. doi: 10.1016/j.snb.2008.09.010

Shi, L., Xu, Y., and Li, Q. (2010). Controlled fabrication of SnO_2 arrays of well-aligned nanotubes and nanowires. *Nanoscale* 2, 2104–2108. doi: 10.1039/c0nr00279h

Sial, M. A. Z. G., Iqbal, M., Siddique, Z., Nadeem, M. A., Ishaq, M., and Iqbal, A. (2017). Synthesis and time-resolved photoluminescence of SnO_2 nanorods. *J. Mol. Struct.* 1144, 355–359. doi: 10.1016/j.molstruc.2017.05.067

Song, H.-M., Chon, B.-S., Jeon, S.-H., Rai, P., Yu, Y., and Dutta, P. K. (2015). Synthesis of Au@SnO_2 core–shell nanoparticles with controllable shell thickness and their CO sensing properties. *Mater. Chem. Phys.* 166, 87–94. doi: 10.1016/j.matchemphys.2015.09.031

Souhir, B., Sami, G., Hekmet, S., and Abdennaceur, K. (2016). Design, simulation and optimization of a meander micro hotplate for gas sensors. *Trans. Electric. Electron. Mater.* 17, 189–195. doi: 10.4313/TEEM.2016.17.4.189

Stuckert, E., Geiss, R., Miller, C., and Fisher, E.l. (2016). In-depth view of the structure and growth of SnO_2 nanowires and nanobrushes. *ACS Appl. Mater. Interfaces* 8, 22345–22353. doi: 10.1021/acsami.6b06676

Sun, D., Luo, Y., Debliquy, M., and Zhang, C. (2018). Graphene-enhanced metal oxide gas sensors at room temperature: a review. *Beilstein J. Nanotechnol.* 9, 2832–2844. doi: 10.3762/bjnano.9.264

Sun, Y.-F., Liu, S.-B., Meng, F.-L., Liu, J.-Y., Jin, Z., Kong, L.-T., et al. (2012). Metal oxide nanostructures and their gas sensing properties: a review. *Sensors* 12, 2610–2631. doi: 10.3390/s120302610

Suzuki, Y., and Yoshikawa, S. (2004). Synthesis and thermal analyses of TiO_2-derived nanotubes prepared by the hydrothermal method. *J. Mater. Res.* 19, 982–985. doi: 10.1557/JMR.2004.0128

Tan, L., Wang, L., and Wang, Y. (2011). Hydrothermal synthesis of SnO_2 sanostructures with different morphologies and their optical properties. *J. Nanomater.* 2011:529874. doi: 10.1155/2011/529874

Thong, L. V., Loan, L. T. N., and Hieu, N. V. (2010). Comparative study of gas sensor performance of SnO_2 nanowires and their hierarchical nanostructures. *Sens. Actuators B* 150, 112–119. doi: 10.1016/j.snb.2010.07.033

Tonezzer, M., Izidoro, S., Areias, J., and Le, T. T. D. (2019). Improved gas selectivity based on carbon modified SnO_2 nanowires. *Front. Mater.* 6:277. doi: 10.3389/fmats.2019.00277

Tong, X., Shen, W., and Chen, X. (2019). Enhanced H_2S sensing performance of cobalt doped free-standing TiO_2 nanotube array film and theoretical simulation based on density functional theory. *Appl. Surf. Sci.* 469, 414–422. doi: 10.1016/j.apsusc.2018.11.032

Tong, X., Shen, W., Chen, X., and andCorriou, J.-P. (2017). A fast response and recovery H_2S gas sensor based on free-standing TiO_2 nanotube array films prepared by one-step anodization method. *Ceramics Int.* 43, 14200–14209. doi: 10.1016/j.ceramint.2017.07.165

Tricoli, A., Righettoni, M., and Teleki, A. (2010). Semiconductor gas sensor: dry synthesis and application. *Angew. Chem. Int. Ed.* 49, 7632–7659. doi: 10.1002/anie.200903801

Tripathy, S., Mishra, A., Jha, S., Wahab, R., and Al-Khedhairy, A. (2013). Synthesis of thermally stable monodispersed Au@SnO_2 core–shell structure nanoparticles by a sonochemical technique for detection and degradation of acetaldehyde. *Anal. Methods* 5, 1456–1462. doi: 10.1039/c3ay26549h

Varghese, O. K., Gong, D., Paulose, M., Ong, K. G., and Grimes, C. A. (2003). Hydrogen sensing using titania nanotubes. *Sens. Actuators B* 93, 338–344. doi: 10.1016/S0925-4005(03)00222-3

Viet, P. V., Phan, B. T., Hieu le, V., and Thi, C. M. (2015). The effect of acid treatment and reactive temperature on the formation of TiO_2 nanotubes. *J. Nanosci. Nanotechnol.* 15, 5202–5206. doi: 10.1166/jnn.2015.10025

Wang, C., Yin, L., Zhang, L., Xiang, D., and Gao, R. (2010). Metal oxide gas sensors: sensitivity and influencing factors. *Sensors* 10, 2088–2106. doi: 10.3390/s100302088

Wang, D., Zhou, W., Hu, P., Guan, Y., Chen, L., Li, J., et al. (2012). High ethanol sensitivity of Palladium/TiO_2 nanobelt surface heterostructures dominated by enlarged surface area and nano-Schottky junctions. *J. Colloid Interface Sci.* 388, 144–150. doi: 10.1016/j.jcis.2012.08.034

Wang, Q., Kou, X., Liu, C., Zhao, L., Lin, T., Liu, T., et al. (2018). Hydrothermal synthesis of hierarchical CoO/SnO_2 nanostructures for ethanol gas sensor. *J. Colloid Interface Sci.* 513, 760–766. doi: 10.1016/j.jcis.2017.11.073

Wang, Y.-L., Guo, M., Zhang, M., and Wang, X.-D. (2010). Hydrothermal preparation and photoelectrochemical performance of size-controlled SnO_2 nanorod arrays. *CrystEngComm* 12, 4024–4027. doi: 10.1039/c0ce00201a

Wang, Z., Haidry, A. A., Xie, L., Zavabeti, A., Li, Z., Yin, W., et al. (2020). Acetone sensing applications of Ag modified TiO_2 porous nanoparticles synthesized via facile hydrothermal method. *Appl. Surf. Sci.* 533:147383. doi: 10.1016/j.apsusc.2020.147383

Wang, Z., Li, Z., Sun, J., Zhang, H., Wang, W., Zheng, W., et al. (2010). Improved hydrogen monitoring properties based on p-NiO/n-SnO_2 heterojunction composite nanofibers. *J. Phys. Chem C* 114 , 6100–6105. doi: 10.1021/jp9100202

Wei, G., Tang, N., He, K., Hu, X., Li, M., and Li, K. (2020). Gas-sensing performances of metal oxide nanostructures for detecting dissolved gases: a mini review. *Front. Chem.* 8:76. doi: 10.3389/fchem.2020.00076

Wilson, A. D., and Baietto, M. (2009). Applications and advances in electronic-nose technologies. *Sensors* 9, 5099–5148. doi: 10.3390/s90705099

Woo, H.-S., Na, C. W., and Lee, J.-H. (2016). Design of highly selective gas sensors via physicochemical modification of oxide nanowires: overview. *Sensors* 1531, 1–23. doi: 10.3390/s16091531

Xia, Y., Li, R., Chen, R., Wang, J., and Xiang, L. (2018). 3D architectured graphene/metal oxide hybrids for gas sensors: a review. *Sensors* 18:1456. doi: 10.3390/s18051456

Xing, X., Chen, N., Yang, Y., Zhao, R., Wang, Z., Wang, Z., et al. (2018). Pt-functionalized nanoporous TiO_2 nanoparticles with enhanced gas sensing performances toward acetone. *Phys Status Solidi* A 215:1800100. doi: 10.1002/pssa.201800100

Xu, C., and Gao, D. (2012). Two-stage hydrothermal growth of long ZnO nanowires for efficient TiO_2 nanotube-based dye-sensitized solar cells. *J. Phys. Chem. C* 116, 7236–7241. doi: 10.1021/jp300960r

Yamazoe, N. (1991). New approaches for improving semiconductor gas sensors. *Sens. Actuators B* 5, 7–19. doi: 10.1016/0925-4005(91)80213-4

Yang, X., Fu, H., Zhang, L., An, X., Xiong, S., Jiang, X., et al. (2019). Enhanced gas sensing performance based on the fabrication of polycrystalline Ag@TiO_2 core-shell nanowires. *Sens. Actuators B* 286, 483–492. doi: 10.1016/j.snb.2019.01.096

Yang, Z., Zhang, Z., Liu, K., Yuan, Q., and Dong, B. (2015). Controllable assembly of SnO_2 nanocubes onto TiO_2 electrospun nanofibers towards humidity sensing applications. *J. Mater. Chem. C* 3, 6701–6708. doi: 10.1039/C5TC01171J

Yin, X.-T., Zhou, W.-D., Li, J., Lv, P., Wang, Q., Wang, D., et al. (2019). Tin dioxide nanoparticles with high sensitivity and selectivity for gas sensors at sub-ppm level of hydrogen gas detection. *J. Mater. Sci.* 30, 14687–14694. doi: 10.1007/s10854-019-01840-w

Yu, K., Wu, Z., Zhao, Q., Li, B., and Xie, Y. (2008). High-temperature-stable Au@SnO_2 core/shell supported catalyst for CO oxidation. *J. Phys. Chem. C* 112, 2244–2247. doi: 10.1021/jp711880e

Zakrzewska, K., Radecka, M., and Rekas, M. (1997). Effect of Nb, Cr, Sn additions on gas sensing properties of TiO_2 thin films. *Thin Solid Films* 310, 161–166. doi: 10.1016/S0040-6090(97)00401-X

Zeng, W., Liu, T., and Wang, Z. (2012). Enhanced gas sensing properties by SnO_2 nanosphere functionalized TiO_2 nanobelts. *J. Mater. Chem.* 22, 3544–3548. doi: 10.1039/c2jm15017d

Zhang, J., Li, C., and Wang, B. (2017). Ag-decorated SnO_2 nanorods: microwave-assisted green synthesis and enhanced ethanol gas sensing properties. *Micro Nano Lett.* 12, 245–247. doi: 10.1049/mnl.2016.0564

Zhang, J., Tu, J., Tang, H., Li, L., Wang, X., and Gu, C. (2014). Hierarchical SnO_2@NiO core/shell nanoflake arrays as energy-saving electrochromic materials. *J. Mater. Chem. C* 2, 10409–10417. doi: 10.1039/C4TC02204A

Zhang, R., Xu, Z., Zhou, T., Fei, T., Wang, R., and Zhang, T. (2019). Improvement of gas sensing performance for tin dioxide sensor through construction of nanostructures. *J. Colloid Interface Sci.* 557, 673–682. doi: 10.1016/j.jcis.2019.09.073

Zhang, X., Lan, W., Xu, J., Luo, Y., Pan, J., Liao, C., et al. (2019a). ZIF-8 derived hierarchical hollow ZnO nanocages with quantum dots for sensitive ethanol gas detection. *Sens. Actuators B* 289, 144–152. doi: 10.1016/j.snb.2019.03.090

Zhang, X., Peng, S., Hong, P., Zha, R., Yang, Y., Xing, X., et al. (2019b). Gas response enhancement of VOCs sensor based on Sn doped nanoporous anatase TiO_2 nanoparticles at a relative low operating temperature. *Mater. Res. Express* 6:105008. doi: 10.1088/2053-1591/ab3516

Zhao, P.-J., Wu, R., Hou, J., Chang, A.-,m., Guan, F., and Zhang, B. (2012). One-step hydrothermal synthesis and visible-light photocatalytic activity of ultrafine Cu-nanodot-modified TiO_2 nanotubes. *Acta Physico-Chim. Sinica* 28, 1971–1977. doi: 10.3866/PKU.WHXB201206111

Zhao, T., Qiu, P., Fan, Y., Yang, J., Jiang, W., and Wang, L. (2019). Hierarchical branched mesoporous TiO_2-SnO_2 nanocomposites with well-defined n–n heterojunctions for highly efficient ethanol sensing. *Adv. Sci.* 6:1902008. doi: 10.1002/advs.201902008

Zhu, S., Zhang, D., Gu, J., Dong, J., and Li, J. (2010). Biotemplate fabrication of SnO_2 nanotubular materials by a sonochemical method for gas sensors. *J. Nanoparticle Res.* 12, 1389–1400. doi: 10.1007/s11051-009-9684-0

Zou, R., Hu, J., Zhang, Z., Chen, Z., and Liao, M. (2011). SnO_2 nanoribbons: excellent field-emitters. *CrystEngComm* 13, 2289–2293. doi: 10.1039/c0ce00543f

Conflict of Interest: The authors declare that the research was conducted in the absence of any commercial or financial relationships that could be construed as a potential conflict of interest.